Sulfate deposition in subsurface regolith in Gusev crater, Mars

Alian Wang,[1] L. A. Haskin,[1,2] S. W. Squyres,[3] B. L. Jolliff,[1] L. Crumpler,[4] R. Gellert,[5] C. Schröder,[6] K. Herkenhoff,[7] J. Hurowitz,[8] N. J. Tosca,[8] W. H. Farrand,[9] Robert Anderson,[10] and A. T. Knudson[11]

Received 19 June 2005; revised 26 October 2005; accepted 28 October 2005; published 21 February 2006.

[1] Excavating into the shallow Martian subsurface has the potential to expose stratigraphic layers and mature regolith, which may hold a record of more ancient aqueous interactions than those expected under current Martian surface conditions. During the Spirit rover's exploration of Gusev crater, rover wheels were used to dig three trenches into the subsurface regolith down to 6–11 cm depth: Road Cut, the Big Hole, and The Boroughs. A high oxidation state of Fe and high concentrations of Mg, S, Cl, and Br were found in the subsurface regolith within the two trenches on the plains, between the Bonneville crater and the foot of Columbia Hills. Data analyses on the basis of geochemistry and mineralogy observations suggest the deposition of sulfate minerals within the subsurface regolith, mainly Mg-sulfates accompanied by minor Ca-sulfates and perhaps Fe-sulfates. An increase of Fe_2O_3, an excess of SiO_2, and a minor decrease in the olivine proportion relative to surface materials are also inferred. Three hypotheses are proposed to explain the geochemical trends observed in trenches: (1) multiple episodes of acidic fluid infiltration, accompanied by in situ interaction with igneous minerals and salt deposition; (2) an open hydrologic system characterized by ion transportation in the fluid, subsequent evaporation of the fluid, and salt deposition; and (3) emplacement and mixing of impact ejecta of variable composition. While all three may have plausibly contributed to the current state of the subsurface regolith, the geochemical data are most consistent with ion transportation by fluids and salt deposition as a result of open-system hydrologic behavior. Although sulfates make up >20 wt.% of the regolith in the wall of The Boroughs trench, a higher hydrated sulfate than kieserite within The Boroughs or a greater abundance of sulfates elsewhere than is seen in The Boroughs wall regolith would be needed to hold the structural water indicated by the water-equivalent hydrogen concentration observed by the Gamma-Ray Spectrometer on Odyssey in the Gusev region.

Citation: Wang, A., et al. (2006), Sulfate deposition in subsurface regolith in Gusev crater, Mars, *J. Geophys. Res.*, *111*, E02S17, doi:10.1029/2005JE002513.

1. Introduction

[2] The Mars Exploration Rover (MER) Spirit landed in Gusev crater on Mars on 3 January 2004. During the primary mission (through sol 90) [*Arvidson et al.*, 2004; *Haskin et al.*, 2005; *Squyres et al.*, 2004; *Yen et al.*, 2005], extensive investigations of soil targets near the landing site and on the impact ejecta of Bonneville crater were made, including surface soils, regolith exposed in the tracks of rover wheels, and the regolith within the Road Cut trench at Laguna Hollow. For these investigations, correlated measurements were made with all instruments of the Athena payload on the same target [*Squyres et al.*, 2003], including two remote sensing instruments, Pancam [*Bell et al.*, 2003] and Mini-TES [*Christensen et al.*, 2003], and three in situ instruments, the Microscopic Imager [*Herkenhoff et al.*, 2003] Mössbauer Spectrometer [*Klingelhöfer et al.*, 2003] and Alpha-Particle X-ray Spectrometer [*Rieder et al.*, 2003], to obtain comprehensive information on soil and rock textures, mineralogy and geochemistry.

[1]Department of Earth and Planetary Sciences, Washington University, St. Louis, Missouri, USA.
[2]Deceased 24 March 2005.
[3]Department of Astronomy, Cornell University, Ithaca, New York, USA.
[4]New Mexico Museum of Natural History and Science, Albuquerque, New Mexico, USA.
[5]Abteilung Kosmochemie, Max-Planck-Institut für Chemie, Mainz, Germany.
[6]Institut für Anorganische und Analytische Chemie, Johannes Gutenberg-Universität, Mainz, Germany.
[7]U. S. Geological Survey, Flagstaff, Arizona, USA.
[8]Department of Geosciences, State University of New York, Stony Brook, New York, USA.
[9]Space Science Institute, Boulder, Colorado, USA.
[10]Jet Propulsion Laboratory, California Institute of Technology, Pasadena, California, USA.
[11]Department of Geological Sciences, Arizona State University, Tempe, Arizona, USA.

0148-0227/06/2005JE002513$09.00

[3] During the early part of the extended mission (sols 91 to 156), the Spirit rover traveled ~2.3 km across the plains from the southeastern rim of Bonneville crater and arrived at the West Spur, a northwestward projecting salient at the foot of the Columbia Hills. A fast traverse was designed for this part of the mission to save time and rover resources for investigation of the Columbia Hills. Nevertheless, Spirit conducted systematic science observations during this traverse at regular four-sol intervals, including near- and mid-field rock surveys [*Crumpler et al.*, 2005], investigation of the thermophysical properties of soils [*Fergason et al.*, 2006], and a series of observations on surface soils and on shallow regolith exposed in rover tracks (A. T. Knudson and P. R. Christensen, Making tracks in Gusev crater: Mini-TES derived mineralogy of near-surface soils at the Mars Exploration Rover Spirit landing site, manuscript in preparation, 2006; hereinafter referred to as Knudson and Christensen, manuscript in preparation, 2006). In addition, Spirit dug two trenches on sol 113 and sol 135, followed by detailed investigation of the regolith within the trenches (Figure 1) [*Haskin et al.*, 2005; *Wang et al.*, 2005b; *Wang et al.*, 2004].

[4] Undisturbed "as is" surface soil observations provide chemical and mineralogical information on the soils to depths of several to tens of micrometers by APXS [*Rieder et al.*, 2003], less than 3 mm by Mössbauer spectroscopy [*Klingelhöfer et al.*, 2003], less than a few micrometers by Pancam Vis-NIR spectroscopy [*Bell et al.*, 2004], and a few tens of micrometers by Mini-TES [*Christensen and Harrison*, 1993]. In the tracks of rover wheels, about a cm of subsurface materials was exposed and investigated. Trench operations, however, reached to substantially greater depths (~10 cm) in the regolith and exposed potential stratigraphic layers. At Gusev, Spirit dug three trenches on the plains before reaching the Columbia Hills (Figure 1). The investigation of regolith at a trench site typically took 3–5 sols to accomplish.

[5] A primary motivation for our investigation of the trenches was to provide ground truth for the Mars Odyssey orbital Gamma-Ray Spectrometer (GRS) instrument [*Boynton et al.*, 2002]. That instrument, which measures gamma radiation produced by cosmic ray interactions and natural radionuclides, determines bulk elemental composition over the upper few tens of cm of the Martian regolith. In situ measurements from the Athena instrument payload can be compared most usefully to GRS data if they are made at comparable depths below the surface.

[6] All surface soils at Gusev measured though sol 156 show very similar geochemical signatures [*Yen et al.*, 2005]. The shallow subsurface regolith exposed in rover wheel tracks is distinct from surface regolith, but different examples of these shallow regoliths are similar to each other in most respects (Knudson and Christensen, manuscript in preparation, 2006). The subsurface regolith within two of the three trenches, the Big Hole and The Boroughs, is distinguished by the deposition of Mg-rich sulfates, the topic of this paper.

2. Trenches and Trench Regolith Investigations

[7] Trenching with rover wheels is useful for exposing subsurface regolith on Mars. The primary goal of MER wheel-trenching activities is to expose near-subsurface material for inspection by the science payload, although some soil mechanics information is also obtained. The same wheel-trenching procedure, with minor variations, was used for digging all three trenches discussed in this paper. The wheel trenching sequence involves the rover executing several partial turns-in-place, passing a single front digging wheel back and forth over the trenching target many times. At various places along the trace of the trench the rover pauses, rotating only a single front wheel either to dig into material, or to move tailings out of the way as the trench deepens, lengthens, and widens. The trenching sequence was optimized to preserve stratigraphic relationships in situ, to minimize contamination of trench interiors by surface materials, and to produce a trench as deep as possible that still is wide enough for IDD instruments to be placed on targets down inside the trench on the floor and facing the (far) wall. Subsurface materials were exposed also on tailings piles deposited on the surface at both ends of each trench (Figure 2).

[8] The first trench, "Road Cut," at Gusev was dug on sol 47 during the primary mission at Laguna Hollow, a 10-m diameter small impact crater located at the boundary of the impact ejecta from Bonneville crater, ~203 m from the rim (Figures 1b and 1c). The trench was ~6–7 cm deep (Figure 2a). In situ measurements using the Microscopic Imager (MI), Mössbauer Spectrometer (MB), and Alpha-Particle X-ray Spectrometer (APXS) were made on the undisturbed soil target "Trout1" before the trench activity. After the trench was dug, long integration MB and APXS measurements were made on a target "Floor3" on the trench floor, and on a target "WallMIonly1" on the trench wall. Stereo microscopic images [*Herkenhoff et al.*, 2004] were taken on the same MB and APXS target on the trench floor, and of four targets on the trench wall to compensate for focusing difficulties associated with roughness of the trench walls. Multispectral Pancam images and Mini-TES spectra were taken on the undisturbed soil, and also on the regolith within the trench and the material excavated by trench operation. The entire Road Cut trench investigation at Laguna Hollow lasted 5 sols (sol 46 to sol 50).

[9] The Big Hole trench and The Boroughs trench were excavated in plains materials between Bonneville crater and

Figure 1. (a) Location of the three trenches along the plains traverse. Concentric circles show the 1, 2, and 3 crater radius distances from the larger impact craters near the traverse route. Note that the Big Hole and The Boroughs trenches are located at a significant distance from nearby larger impact craters. (b) Pretrench and (c) posttrench views of Laguna hollow, a 10 m diameter impact crater on the distal edge of the continuous ejecta deposits from Bonneville crater. (d). The approximate location of the Big Hole trench in the plains between Missoula and Lahontan craters. View is directed approximately N13°E. (e) View of surrounding plains from the location of The Boroughs trench. This trench was more distally located with respect to recent impact ejecta and lies within a featureless region.

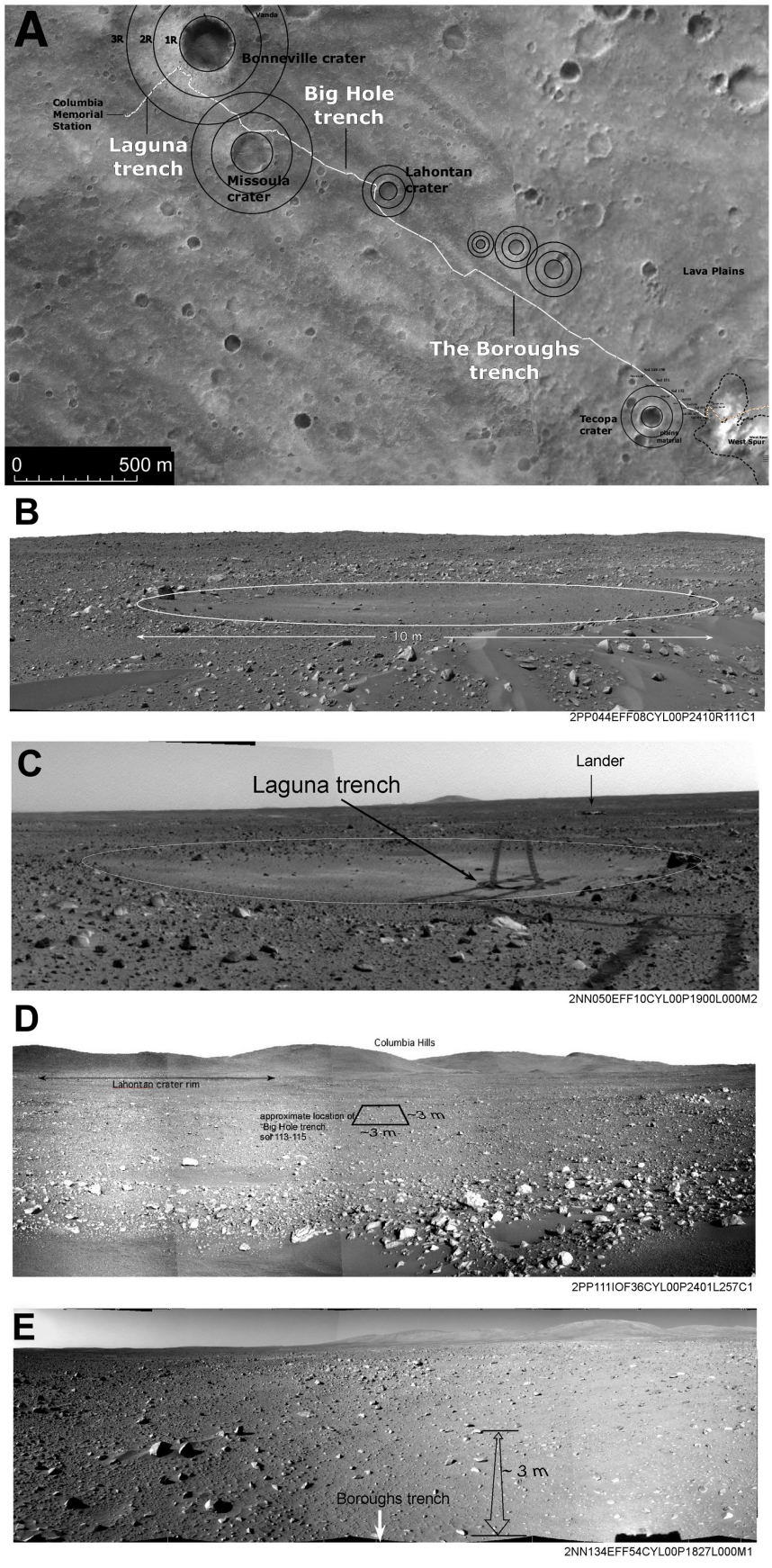
A
3R
2R
1R
Bonneville crater
Columbia Memorial Station
Big Hole trench
Laguna trench
Missoula crater
Lahontan crater
Lava Plains
The Boroughs trench
Tecopa crater
West Spur
0
500 m
B
~10 m
2PP044EFF08CYL00P2410R111C1
C
Laguna trench
Lander
2NN050EFF10CYL00P1900L000M2
D
Columbia Hills
Lahontan crater rim
approximate location of Big Hole trench sol 113-115
~3 m
~3 m
2PP111IOF36CYL00P2401L257C1
E
~3 m
Boroughs trench
2NN134EFF54CYL00P1827L000M1

Figure 1

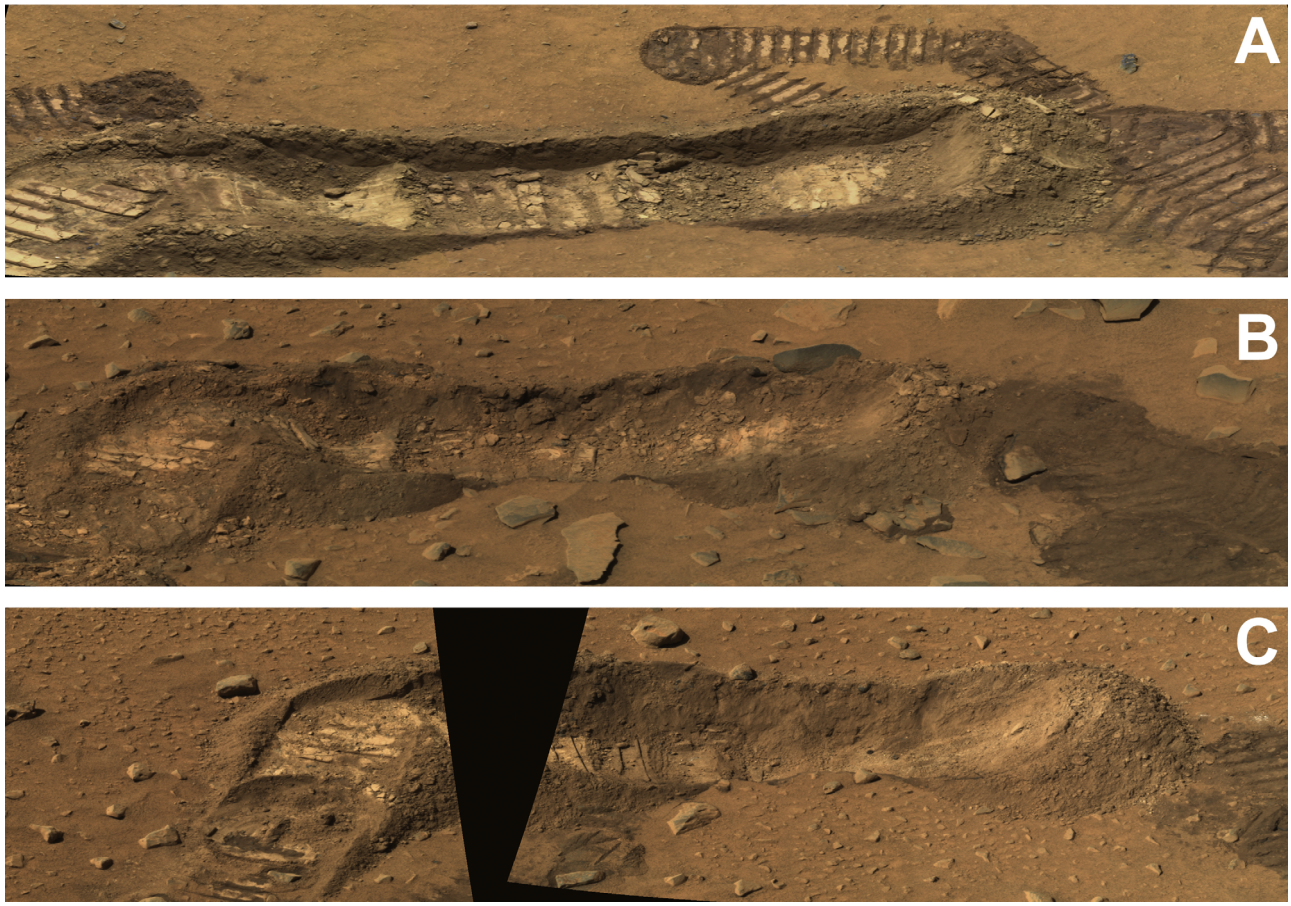

Figure 2. True color Pancam images of three trenches: (a) Road Cut trench at Laguna Hollow (203 m from Bonneville Crater rim, 6–7 cm deep); (b) Big Hole trench in the plains (556 m from Bonneville Crater rim, ~9 cm deep); and (c) The Boroughs trench in the plains (1698 m from Bonneville Crater rim, ~11 cm deep).

the Columbia Hills. The Big Hole trench is ~556 m away from the rim of Bonneville crater, and The Boroughs trench is ~1698 m away (Figures 1d and 1e). For the Big Hole trench, the in situ measurements (MI, MB, APXS) on the "as is" undisturbed surface soil target "MayFly" were obtained at the location of the excavation and are considered to be representative of the surface soil in the general area. The excavation made a ~9 cm deep trench (Figure 2b). Coupled MB and APXS measurements were done on a target "RS2" on the floor of the trench, plus an additional APXS on a second target "Trio" on the floor. One set of microscopic images was taken of the floor target "RS2", with 3 sets from trench wall targets. After backing up ~0.85 m, multispectral Pancam images and Mini-TES spectra were taken to cover the area including the trench and its surroundings. The investigation lasted 3 sols (sol 113 to sol 115).

[10] At the Boroughs trench, the target "SeattleSlew" was chosen for the pretrench surface measurements (MI, MB, APXS). This target was on disturbed soil within a rover track, about 3 m away from the exact excavation location of the trench. The excavation made a ~11 cm deep trench (Figure 2c). Light-toned regolith was excavated from the trench and observed on the upper portion of the trench wall, but dark-toned regolith was observed on the trench floor. The coupled MB and APXS measurements after trenching were made on a target "Millbasin" on the trench floor and a target "HellsKitchen" on the trench wall (Figure 3), with one set of MI images from the floor target and three sets from wall targets. After backing up, multispectral Pancam images and Mini-TES spectra were taken to cover The Boroughs trench and its surroundings. Spirit stayed at the location for a total of eight sols because of a spacecraft fault. The actual investigation of The Boroughs trench lasted 4 sols. Additional details on the investigations for each of these three trenches are listed in Table 1.

3. Measurement Results

3.1. Road Cut Trench at Laguna Hollow

[11] Both Mini-TES [*Christensen et al.*, 2004] and Mössbauer spectral analyses [*Morris et al.*, 2004] of the Road Cut trench indicate a basaltic mineralogy for the regolith at the top and within the trench, i.e., olivine, pyroxene, feldspar, and iron oxides such as nonstoichiometric magnetite and nanophase ferric oxides (a group of fine-grained, <10 nm, poorly crystalline phases considered a general alteration product of plains basalts at Gusev. Nanophase oxides can include the superparamagnetic

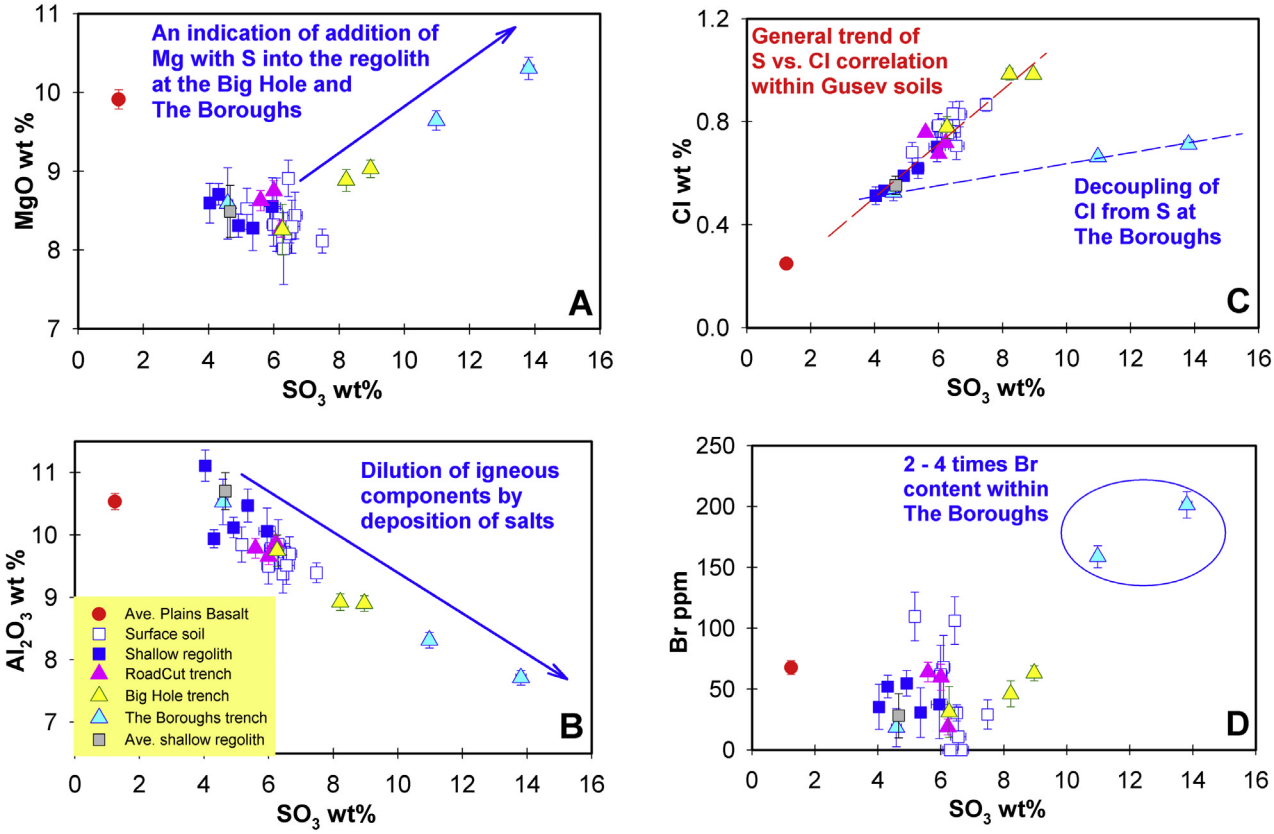

Figure 3. Compositional correlations within the regolith materials at Gusev (APXS data through sol 158): (a) MgO versus SO_3; (b) Al_2O_3 versus SO_3; (c) Cl versus SO_3; and (d) Br versus SO_3.

forms of Fe-oxides, oxyhydroxides, sulfates, and the Fe^{3+} pigment in palagonitic tephra [*Morris et al.*, 2000, 2004]) (Table 2). Basaltic mineralogy is also consistent with normative calculations [*Wang et al.*, 2004] on the basis of compositional chemistry obtained by APXS measurements [*Gellert et al.*, 2004]. The compositional data further show that the wall and floor regolith are indistinguishable from that of typical shallow subsurface soils measured in the rover wheel tracks.

[12] Surprisingly, Mini-TES data in trenches on Mars are not dominated by black body effects due to the cavity created by the trench. The thermal infrared spectral signatures of materials in the Road Cut trench and disturbed soils in tracks adjacent to the trench are consistent with a basaltic mineralogy. The dust-free fraction is made up of ~45% feldspar, ~40% pyroxene, and ~10% olivine with an additional 5% sulfates. There are minor differences in spectral shape and retrieved mineralogy between the track to the right of the trench and the materials within the trench, but these variations are within the noise of the data set. The trench materials are also similar to a representative disturbed soil observation taken in a rover track on sol 089. The derived mineralogy of the track is ~45% pyroxene, ~40% plagioclase, and ~15% olivine [*Christensen et al.*, 2004]. Although the differences between these mineral results are within the limits of Mini-TES detection and the deconvolution mineral retrieval (5–10%), the increased olivine and pyroxene in the track is likely to represent real variability. These minerals have distinct absorption features in the long wavelengths, where the spectral shapes clearly differ (Figure 4a).

[13] The 20 mrad spot size of the Mini-TES field of view is approximately the same size as the whole wall or the floor of the trench (Figure 4b). Since Mini-TES views the trench at an oblique angle, each field of view inside the trench covers the visible floor and about half of the far wall. Spectra are representative of the average relative area abundance of minerals over this whole area. In observations of the near-by tracks, it is clear that they contain some amount of dust compacted into the soil and may also include pebbles pressed into the tracks.

[14] In the Vis-NIR spectra extracted from the multispectral Pancam images (Figure 5a), the spectrum of surface soil has a blue to red slope higher than the subsurface regolith, which suggests a higher oxidation state [*Farrand et al.*, 2006]. This observation is supported by Fe^{3+}/Fe_{TOTAL} values from Mössbauer data (0.30 at surface and 0.22–0.23 for subsurface regolith, Table 2). In addition, multispectral Pancam images show that this oxidized surface layer is very thin (~1 mm). Because the penetration depth of the Mössbauer signal can reach ~3 mm in loose dust, the oxidation state of the surface soils could be even higher than the reported value (Fe^{3+}/Fe_{TOTAL} ~ 0.30), because part of the Mössbauer signal comes from the underlying regolith which is generally lower in Fe^{3+}/Fe_{TOTAL}. In addition, there

Table 1. Trench Investigations at Gusev by Spirit

Sol	Instrument	Targets and Name
	Road Cut Trench at Laguna Hollow	
046	MI (7 positions + stereo)	PreMB_Trout1
	MB (12 hrs)	Surface soil_Trout1
	APXS (5 hrs)	Surface soil _Trout1
047	Rover trench (6–7 cm depth)	
	MTES (9 × 5 × 20 s raster)	Road Cut_trench
	Pcam (4x2 mosaic L257R1)	Road Cut_trench
048	MI (7 positions + stereo)	TrenchWall_RoadCut_WallMIonly1
	MI (7 positions + stereo)	TrenchWall_RoadCut_WallMIonly2 (1 cm below)
	MI (7 positions + stereo)	TrenchFloor_Floor3
	MB (12 hrs)	Trench Floor _RoadCut_Floor3
	APXS (8 hrs)	Trench Floor _RoadCut_Floor3
049	MI (7 positions + stereo)	Trench Floor _RoadCut_Floor3_postMB
	MI (7 positions + stereo)	TrenchWall_Roadcut1_DividingLine
	MI (7 positions + stereo)	TrenchWall_Roadcut2_MasonDixon
	MI (7 positions + stereo)	TrenchWall_Roadcut_Wall3
	MB (12 hrs)	Trench wall_MIonly1
	APXS (10 hrs)	Trench wall_MIonly1
050	MI (3 positions)	Trench Wall_Roadcut_Mionly_PostMB
	MI (3 positions)	Roadcut_Mason Dixon
	Rover backup ~0.85 m	
	Pcam (4x1, 13 filters)	Road Cut_trench
	MTES (9 × 3 × 20 raster)	Road Cut_trench
	MTES (40s stare)	
	Big Hole Trench	
113	APXS (38 min)	MayFly surface
	MB (2 hrs)	MayFly surface
	MI (3 positions)	MayFly surface
	Rover bump back	
	Rover Trench (~9 cm depth)	
114	MI (5 positions)	TrenchWall_Stonefly
	MI (5 positions)	TrenchWall_ Brassie
	MI (3 positions)	TrenchFloor_RS2
	MI (3 positions)	Post MB on RS2
	APXS (12 hrs)	TrenchFloor_RS2
	APXS (4.5 hrs)	TrenchFloor_Trico
115	MI (5 positions)	TrenchWall_Stonefly
	Rover bump back ~0.85 m	
	Pcam (4 × 1, 13 filters)	Big Hole trench
	MTES (9 × 3 × 20 raster)	Big Hole trench
	The Boroughs Trench	
135	APXS (35 min)	SantaAnita_Seattle Slew (in track)
	MB (2 hrs)	SantaAnita_Seattle Slew
	MI (5 Positions)	SantaAnita_Seattle Slew
	Rover approach	
	Rover trench (~11 cm depth)	
140	MB (5.5 hrs)	Trench floor_Mill Basin
	APXS (9.3 hrs)	Trench floor_Mill Basin
	APXS (5.4 hrs)	Trench wall_Hells Kitchen
141	MI (5 positions)	Trench floor_Mills3
	MI (6 positions + stereo)	Trench wall _Forham
	MI (6 positions + stereo)	Trench wall _Kew_Gardens
	MB (3 hrs)	Trench wall _Hells Kitchen
	MI (3 positions)	Trench wall _Hells Kitchen
	Rover bump back ~0.85 m	
	MTES (19 × 5 × 20 raster)	The Boroughs trench
142	Pcam (4 × 1, 13 and 5 filters)	The Boroughs trench

may be highly oxidized species (other than Fe^{3+}) that cannot be "seen" by the Mössbauer spectrometer within the top surface dust that were products of photochemical reactions occurring at reactive mineral surfaces [*Yen et al.*, 2000]. Table 2 shows that the higher oxidation state of the surface dust corresponds to an increase in the abundance of nanophase ferric oxides and slight reductions of ferrous olivine and ferrous pyroxene. The microscopic images (Figure 6a) show homogeneous, sand-sized grains in the subsurface regolith within the trench, which supports aeolian origin, i.e., wind-blown sands.

[15] Morphologic arguments (Figures 1b and 1c) suggest that aeolian transport is the primary process responsible for infilling of small craters like Laguna Hollow [*Golombek et al.*, 2006; *Grant et al.*, 2006]. The consistency in the depth profiles of the oxidation states at Road Cut trench and at other locations (disturbed or undisturbed) throughout the Gusev plains, and the homogeneity in compositional

Table 2. Mössbauer Spectral Analysis Results for the Regolith in Three Trenches on the Gusev Plains[a]

	Fe^{2+}_Ol (%)	Fe^{2+}_Px (%)	Fe^{3+}_np (%)	$Fe^{2+}Fe^{3+}$_Mt (%)	Fe^{3+}_Hm (%)	Fe^{3+}/Fe_T
Road Cut Trench at Laguna Hollow						
As is surface (Trout1)	36	31	20	9	4	0.30
Trench Wall (Ml only)	38	37	15	8	1	0.23
Trench Floor (floor3)	38	37	15	9	1	0.23
Big Hole Trench						
As is surface (MayFly)	41	30	18	11	0	0.26
Trench Floor (RS2)	28	27	37	8	1	0.44
The Boroughs Trench						
Surface In track (Seattle Slew)	34	38	18	9	2	0.26
Trench Wall (Hells Kitchen)	27	29	34	9	1	0.42
Trench Floor (Mill Basin)	30	31	29	8	2	0.36

[a]Component uncertainties are ±2% absolute; Fe^{3+}/Fe_T uncertainty is ±0.03 (f-factor corrected). Ol, olivine; Px, pyroxenes; np, nanophase Fe^{3+}oxide; Mt, nonstoichiometric magnetite; Hm, hematite.

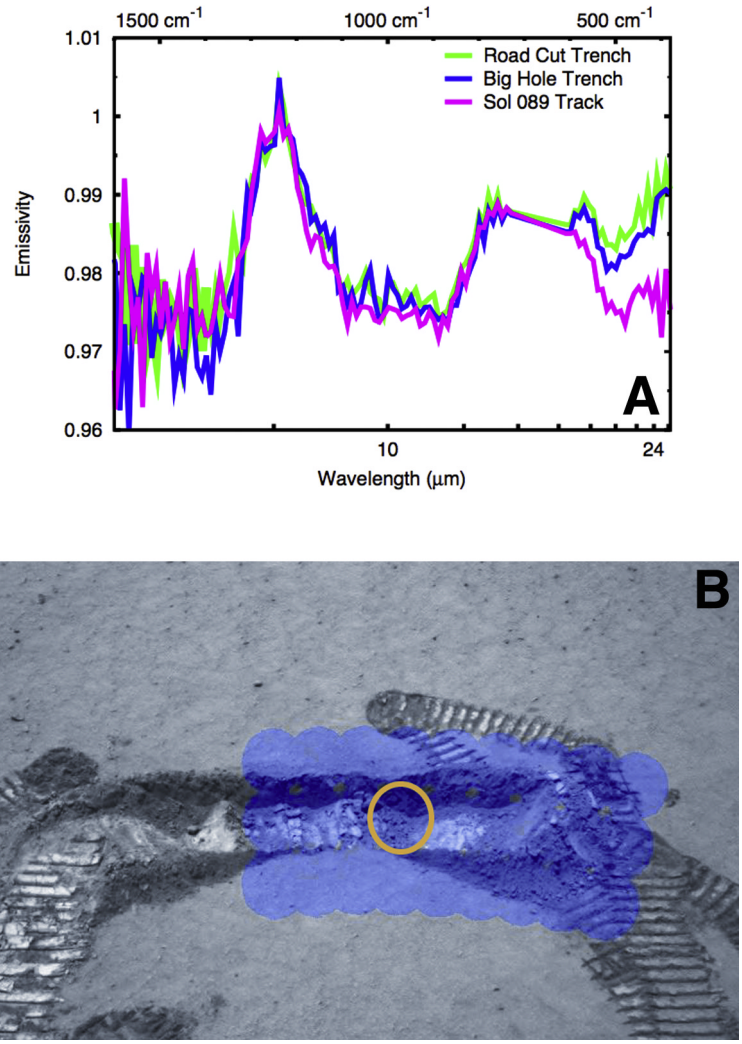

Figure 4. (a) Mini-TES spectra extracted from observations of Road Cut trench (sequence p3161, sol 050), Big Hole trench (sequence p3236, sol 116), and a representative disturbed near-surface soil measured in a rover track on the flank of Bonneville Crater (sequence p3660, sol 089). The track spectrum has been scaled for clarity of comparison. (b) Part of a Navcam frame showing Road Cut trench with the Mini-TES footprints overlaid. One representative pixel is highlighted to emphasize the size of the Mini-TES pixel in relation to the trench.

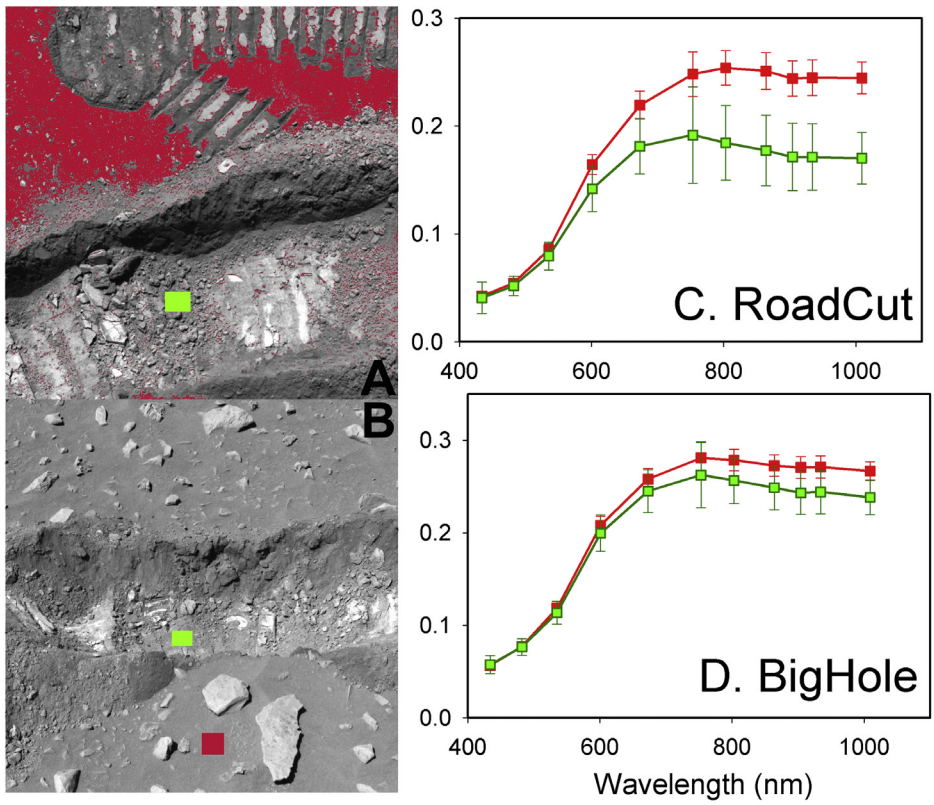

Figure 5. Vis-NIR spectra extracted from multispectral Pancam images: (a) Road Cut trench at Laguna Hollow, the areas within the trenches where the spectra were extracted are color-coded. (b) Big Hole trench in the plains. (c) The spectrum from the uppermost layer of surface soil at Road Cut trench site shows a much higher blue to red slope than the subsurface regolith. (d) At Big Hole trench site, fairly similar blue to red slopes are seen in the spectra from the surface and subsurface regolith.

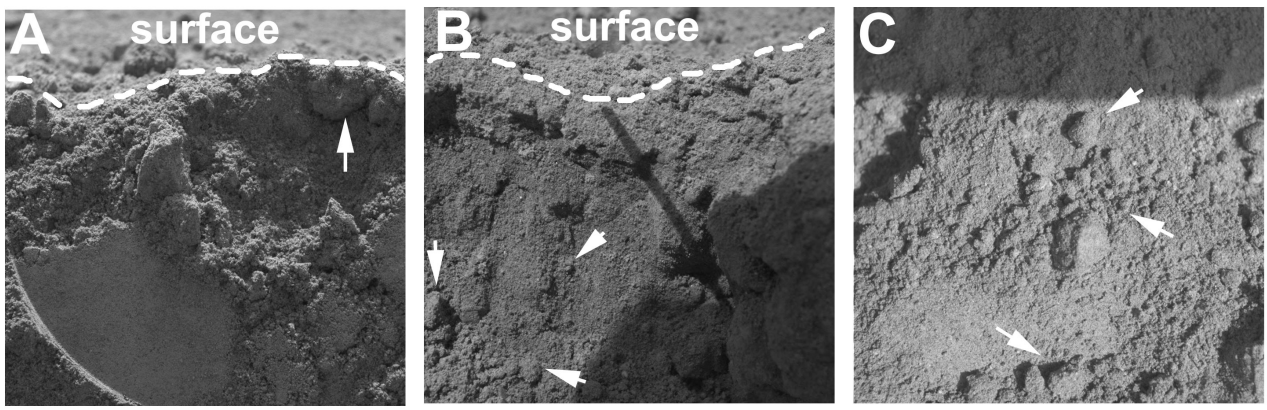

Figure 6. Single frame microscopic images of subsurface regolith within the three trenches (field of view ~3.1 cm for single frame, ~31 mm/pixel). (a) Wall regolith within the Road Cut trench at Laguna Hollow: The image of target "WallMIonly1" was taken on sol 50 post Mössbauer and APXS measurements. The circular depression is the impression of the contact plate of the Mössbauer spectrometer. The sand grains appear to be well-sorted (dust grains cannot be spatially resolved) and consistent with aeolian deposition. Arrows point to the cohesive crusts near the surface. (b) Wall regolith within the Big Hole trench in the plains: The image of target "Stonefly" was taken on sol 116, which was partially shadowed. The needle-shaped shadow is of the MI contact sensor. Note the inhomogeneity in grain sizes and the appearance of grain aggregates (noted by arrows). (c) Floor-regolith within The Boroughs trench in the plains. The image of target "Mills Basin" was taken on sol 141 and was partially shadowed. Note the wide range of grain sizes and the grain aggregates (noted by arrows).

chemistry among the regolith materials within this trench and the general regolith (disturbed and undisturbed) on Gusev plains (Figure 3) both support the hypothesis that physical processes such as impact gardening and aeolian transport are responsible for the origin of the regolith at this trench. The coarse sand-sized materials were brought in by wind and filled in the Laguna Hollow that was originally formed by impact, and highly oxidized fine-grained wind-blown dust has since accumulated at the surface.

3.2. The Big Hole and The Boroughs Trenches

[16] The sites of these two trenches were chosen by the Athena science team to lie within topographically low regions on the plains, in areas of comparatively low thermal inertia (i.e., low rock abundance). They are far removed from larger impact craters (Figures 1a, 1d, and 1e) in order to increase the likelihood that the subsurface regolith exposed by the trenching operation would be relatively mature with regard to weathering and dust accumulation.

[17] Compared to the trench at Laguna Hollow, the regolith sections exposed within Big Hole and The Boroughs trenches exhibit an inverse depth profile of oxidation states, a wide range of compositional variation, tight correlations among elemental compositions, a different Vis-NIR spectrum from the subsurface, and different morphology as seen in microscopic images.

[18] The regolith at depth within Big Hole and The Borough trenches have the highest oxidation state among all Gusev soils measured through sol 400 (Table 2). The near-surface regolith at Big Hole (measured at an "as is" undisturbed surface) and at The Boroughs (measured at a shallow subsurface exposure in the rover track) have Fe^{3+}/Fe_{TOTAL} values (0.26) very similar to general soils (disturbed and undisturbed) at Gusev. However, a Fe^{3+}/Fe_{TOTAL} value of 0.42 was found in the regolith on the wall at The Boroughs trench, with a slightly lower value (0.36) for trench floor regolith but is still much higher than the near-surface regolith. The mineral modes implied by Mössbauer data analysis (Table 2) indicate decreased ferrous iron associated with olivine and pyroxene and increased nanophase ferric oxides [*Morris et al.*, 2005, 2006].

[19] This depth profile of oxidation state at both trenches is supported by Vis-NIR spectra extracted from the multispectral Pancam images (Figure 5b). The blue to red slopes at the absorption edge (~535 nm) in the spectra of regolith on the trench wall and at the trench floor are the same as for surface soils, which suggests that they are not less oxidized than surface soils. The spectrum from the subsurface has a negative slope in the NIR spectral region and a local maximum at ~750 nm, which may indicate Fe^{3+}-bearing hydroxides or sulfates, or ferrous iron in basaltic sand, or all of these possibilities. Light-toned materials were apparently excavated at The Boroughs trench, but the Vis-NIR spectra of these materials do not have specific spectral features that permit their identification.

[20] In the microscopic images of the Big Hole trench wall and The Boroughs trench floor (Figures 6b and 6c), poorly sorted sand, granules, pebbles, and cobbles are seen, which is in contrast to the homogeneous sand sized-grains within the first trench at Laguna Hollow. Rather than an aeolian origin, this characteristic suggests that impact-mixing processes dominated the formation of the subsurface regolith at these two trench sites.

[21] The regolith at The Boroughs trench has the highest S, Br, and Mg concentrations of any soil on the Gusev plains (Table 3, Figure 3). The concentration of Mg within basaltic blocks on the plains typically increases from exterior to interior as the interior is exposed by RAT abrasion [*Haskin et al.*, 2005; *McSween et al.*, 2004]. The maximum concentration is found in the exposed interior of the rock Adirondack, where Mg is apparently associated with high olivine and pyroxene proportions [*McSween et al.*, 2004]. Mg concentrations in surface soils and shallow subsurface regoliths are lower than in rocks [*McSween et al.*, 2004; *Yen et al.*, 2005]. The subsurface regolith within two plains trenches, however, have Mg concentrations 7–25 relative% higher than those of typical Gusev soils. The highest value found on the wall of The Boroughs trench is within the same range of the abraded plains basalt (Adirondack and Humphrey [*Haskin et al.*, 2005, Figure 3]). Moreover, these Mg values are not correlated with other major silicate-related cations (Al, Si, Ca, Fe). On the contrary, a very tight positive correlation of MgO to SO_3 in mass% (r = 0.998), was found from the subsurface regolith measurements within the Big Hole and The Boroughs trenches (Figure 3a), suggesting that Mg has been transported together with S, and deposited as Mg-sulfates in the trench regolith. Because no obvious correlations of CaO to SO_3 or Fe_2O_3 to SO_3 are observed, it is likely that Mg is the major cation in the deposited sulfates. Furthermore, the negative correlations of Al_2O_3 to SO_3 in mass% (r = 0.993, Figure 3b) and SiO_2 to SO_3 in mass% (r = 0.995, not shown) observed from the same data set demonstrate dilution of silicates due to the deposition of sulfates.

[22] The subsurface regolith exposed in the two plains trenches shows unusually high concentrations of the soluble elements S, Cl, and Br (Figures 3c and 3d). More importantly, the relative ratios of these elements are distinct from the typical values found at Gusev, including both surface soils and coatings on rocks. Among all Gusev rock surfaces and soils measured through sol 156, Cl is positively correlated with S (r = 0.961, 34 data points), representing a relatively narrow range of S to Cl molar ratio (~8) in these targets (Figure 3c), which suggests that a similar chemical process controlled the deposition of S and Cl in the typical Gusev soils. The only two exceptions are the multilayered coatings on the rock Mazatzal [*Haskin et al.*, 2005, not shown] and the subsurface regolith within The Boroughs trench (Figure 3c). The latter is double the typical S to Cl molar ratio. The decoupling of S from Cl indicates that different processes may have been involved in the deposition of S and Cl in these trenches.

[23] Elevated Br concentrations were obtained in the interior of the rock Mazatzal, and were interpreted as precipitation in the vugs and veins from the latest stage of brine that penetrated into the rock [*Gellert et al.*, 2004; *Haskin et al.*, 2005]. Br concentrations higher than the interior of Mazatzal were observed from the regolith within The Boroughs trench (Figure 3d).

[24] The Mini-TES spectra from Big Hole trench are similar to Road Cut trench. The retrieved mineral modes are indistinguishable, although there is a minor increase of sulfate abundance to between 5 and 10%; however, this

Table 3. Compositions of Regolith Derived From APXS and Mössbauer Analyses on the Gusev Plains[a]

APXS File	A126 CS		A122, 135, 158S		A047 CS		A049 CS		A050 CS		A113 CS		A114 CS		A115 CS		A135 S		A140 S		A141 S	
Sample	Surface soil		Avg disturbed regolith		Road Cut Top (Trou1)		Road Cut Floor (Floor3)		Road Cut Wall (MI Only)		Big Hole Top (MayFly)		Big Hole Floor (RS2)		Big Hole Floor (Trio)		The Boroughs Top (in track) (Seattle Slew)		The Boroughs Floor (Mill Basin)		The Boroughs Wall (Hells Kitchen)	
	wt%	±	wt%	±	wt%	±	wt%	±	wt%	±	wt%	±	wt%	±	wt%	±	wt%	±	wt%	±	wt%	±
Na_2O	3.06	0.72	3.12	0.49	3.13	0.11	2.44	0.15	2.65	0.14	3.10	0.52	2.51	0.11	2.47	0.15	3.04	0.73	2.36	0.11	2.53	0.14
MgO	8.15	0.46	8.63	0.34	8.41	0.11	8.90	0.13	8.78	0.13	8.40	0.33	9.19	0.11	9.04	0.14	8.74	0.46	9.82	0.13	10.48	0.14
Al_2O_3	10.01	0.4	10.88	0.30	10.04	0.11	9.83	0.14	9.96	0.16	9.91	0.26	9.06	0.13	9.08	0.14	10.70	0.37	8.46	0.13	7.84	0.12
SiO_2	46.25	0.83	47.26	0.70	45.98	0.33	46.17	0.47	46.13	0.47	46.13	0.64	43.68	0.40	44.23	0.47	46.95	0.69	41.36	0.39	39.24	0.40
P_2O_5	0.83	0.1	0.82	0.07	0.86	0.03	0.68	0.03	0.73	0.03	0.88	0.07	0.80	0.03	0.74	0.03	0.77	0.08	0.71	0.03	0.80	0.03
SO_3	6.40	0.24	4.73	0.17	6.32	0.09	6.10	0.09	5.69	0.08	6.36	0.18	9.11	0.10	8.36	0.12	4.66	0.16	11.17	0.12	14.04	0.16
Cl	0.77	0.05	0.56	0.04	0.73	0.02	0.69	0.02	0.77	0.02	0.79	0.04	1.00	0.02	1.00	0.02	0.54	0.03	0.68	0.01	0.73	0.02
K_2O	0.45	0.03	0.45	0.03	0.44	0.01	0.38	0.01	0.37	0.01	0.47	0.03	0.35	0.01	0.34	0.01	0.42	0.02	0.35	0.01	0.36	0.01
CaO	6.50	0.14	6.32	0.12	6.32	0.05	6.14	0.06	6.24	0.05	6.07	0.11	5.74	0.04	5.86	0.06	6.27	0.11	5.77	0.05	5.76	0.05
TiO2	0.96	0.07	0.81	0.06	0.89	0.02	1.00	0.03	1.02	0.02	1.00	0.05	0.87	0.02	0.89	0.02	0.89	0.08	0.90	0.02	0.85	0.03
Cr_2O_3	0.29	0.05	0.37	0.04	0.33	0.01	0.43	0.02	0.40	0.02	0.37	0.04	0.36	0.01	0.43	0.02	0.42	0.04	0.39	0.01	0.39	0.02
MnO	0.32	0.04	0.32	0.03	0.34	0.01	0.34	0.01	0.35	0.01	0.31	0.03	0.34	0.01	0.34	0.02	0.34	0.03	0.36	0.01	0.34	0.01
FeO	11.75	0.19	11.24	0.15	11.27	0.06	12.91	0.10	12.91	0.09	11.90	0.14	9.43	0.06	9.56	0.08	11.94	0.15	11.22	0.07	9.57	0.07
Fe_2O_3	4.59	0.07	4.86	0.06	5.37	0.03	4.29	0.03	4.29	0.03	4.65	0.05	8.24	0.05	8.35	0.07	4.66	0.06	7.01	0.05	7.70	0.06
NiO	0.08	0.02	0.06	0.01	0.04	0.004	0.06	0.01	0.08	0.005	0.06	0.01	0.06	0.003	0.06	0.01	0.06	0.01	0.06	0.004	0.06	0.004
ZnO	0.05	0.01	0.03	0.01	0.04	0.002	0.04	0.003	0.03	0.003	0.02	0.01	0.06	0.002	0.05	0.003	0.04	0.01	0.04	0.002	0.03	0.003
Br	<0.01	0.001	<0.01	0.002	<0.01	0.001	0.01	0.001	0.01	0.001	<0.01	0.002	0.01	0.001	<0.01	0.001	<0.01	0.002	0.02	0.001	0.02	0.001
Sum oxides	100.3		100.3		100.3		100.3		100.2		100.3		100.6		100.6		100.3		100.5		100.6	
Fe^{3+}/Fe_T	0.26[b]		0.28[c]		0.3		0.23		0.23		0.26		0.44		0.44		0.26		0.36		0.42	

[a]Compositions of regolith are in oxides wt%.
[b]No corresponding Mössbauer measurement for this sol, use the value of sol 113.
[c]Averaged over three Mössbauer measurements.

Table 4. Mole Proportions of Remaining Cations and Anions After Subtraction of the Composition of an Average Shallow Regolith From the Wall and the Floor Regolith Within the Big Hole and The Boroughs Trenches

Sample Regolith	Big Hole Floor		The Boroughs Wall		The Boroughs Floor	
	mass%		mass%		mass%	
Ave. Regolith	83.2		71.9		77.8	
Remnant	mole%	±	mole%	±	mole%	±
Na_2O	−0.6	1.9	1.1	2.0	−0.3	2.5
MgO	**20.7**	**2.1**	**25.4**	**2.2**	**23.4**	**2.7**
Al_2O_3	0.0	0.8	0.0	0.8	0.0	1.0
SiO_2	**30.0**	**3.2**	**21.0**	**3.2**	**23.2**	**4.1**
P_2O_5	0.3	0.1	0.3	0.1	0.1	0.2
SO_3	**26.8**	**0.6**	**31.9**	**0.7**	**28.4**	**0.8**
Cl	6.2	0.3	2.2	0.3	2.0	0.3
K_2O	−0.1	0.1	0.1	0.1	0.0	0.1
CaO	**3.5**	**0.5**	**5.2**	**0.5**	**4.6**	**0.7**
TiO_2	1.0	0.2	0.8	0.2	1.0	0.2
Cr_2O_3	0.1	0.1	0.2	0.1	0.2	0.1
MnO	0.5	0.1	0.4	0.1	0.5	0.1
FeO	**0.4**	**0.5**	**4.9**	**0.5**	**10.4**	**0.7**
Fe_2O_3	**10.9**	**0.1**	**6.3**	**0.1**	**6.1**	**0.1**
NiO	0.1	0.0	0.0	0.0	0.1	0.0
ZnO	0.2	0.0	0.0	0.0	0.0	0.0
Br	0.0	0.0	0.1	0.0	0.1	0.0
Total	100		100		100	
MgO/CaO	**5.8**	**1.1**	**4.9**	**0.7**	**5.1**	**0.9**
MgO+CaO	**24.2**	**2.2**	**30.6**	**2.2**	**28.0**	**2.8**

result is well within the uncertainty of spectral deconvolution. The trench soils maintain the basaltic mineralogy measured in Road Cut trench and in tracks. The variation detected in oxidation state and sulfate materials in this trench with the IDD instruments are below the 5–10% uncertainty of Mini-TES, taking into account that the field of view of Mini-TES in this location covers the full wall and floor of the trench. Small areas or horizons of material in the trench with distinctly different compositions are dominated by the composition of bulk local soil. Mini-TES data at the Boroughs trench were acquired at a local true solar time of 16:07. Because the observation was taken at this late time of day, coupled with the fact that the rover shadowed the trench materials while IDD analysis took place, the temperature of materials at the trench is extremely low. The average temperature of this observation is 226 K. The measurements of cold surface materials are dominated by downwelling radiance from the relatively warmer sky. Without extensive modeling of atmospheric contributions these data are not appropriate for spectral analysis.

4. Mineralogy of the Salts and Silicates in Regolith Within Two Trenches on the Plains

[25] Observations hitherto on the plains within Gusev crater suggest that at least the top ~10–11 cm of regolith consists of three main components: (1) the uppermost, undisturbed thin layer (up to a few mm) of dust which has likely been homogenized by aeolian activity, (2) the dust-free regolith at shallow depth exposed by tracks and scuffs made by the rover, and (3) the deeper sulfur-rich regolith (e.g., trench walls and floors) [*Yen et al.*, 2005]. The morphologic, chemical, and mineralogic evidence suggests that the regolith materials at the Road Cut trench site are composed primarily of components (1) and (2), whereas the Big Hole and The Boroughs trenches have exposed component (3).

[26] The mineralogical characteristics of component (3) at the Big Hole and The Boroughs trench sites are important for understanding the geological processes involved in their formation and subsequent reactions, including interaction with water or acidic fluids. We will treat the mineralogy of salts and mineralogy of silicates separately. We typically use four approaches in these analyses: a first-order molar-ratio comparison of the cations and anions; a modified normative calculation; a mass-balance mixing-model calculation; and an olivine mass% calculation using the Fe information from APXS and Mössbauer analyses.

4.1. Mineralogy of Salts: Molar Ratio Comparison and Mixing Model

[27] To a first approximation, molar ratio comparison of the cations and anions was used. We consider the deep regolith within these trenches (component 3) to be made of a common low-sulfur "dust-free" shallow regolith (component 2, using an average of the three measurements made in nearby rover tracks), plus some extra mineral phases contributing to the high-sulfur and alteration signatures that made the deep regolith within the trenches distinct from the others. Therefore, by subtracting a percentage of the shallow regolith composition from that of the wall regolith at The Boroughs (the richest in S) until zero concentration of Al_2O_3 is reached in the remnant (assuming Al_2O_3 is restricted to the silicate portion of the regolith), we can obtain a rough estimate of the "extra" mineral phases in the wall regolith at The Boroughs. Table 4 shows that in the residual composition of the wall regolith so calculated, the sum of MgO and CaO molar percents matches fairly closely the molar percent of SO_3, with an MgO/CaO molar ratio ~4.9 ± 0.7. When calculating cation/anion ratios for the floor regolith at The Boroughs trench, the sum of the number of moles of MgO and CaO also matches the number of moles of SO_3, with an MgO/CaO molar ratio ~5.1 ± 0.9. This approximate calculation suggests strongly that within The Boroughs trench (as well as the Big Hole

Table 5. Results of Mass-Balance Mixing-Model Calculations[a]

	The Big Hole Floor (RS2)			The Boroughs Wall (Hells Kitchen)					The Boroughs Floor (Mill Basin)				
	APXS Composition			APXS Composition			Ten Varied Compositions Within APXS Uncertainties		APXS Composition			Ten Varied Compositions Within APXS Uncertainties	
	mass%	±	± in%	mass%	±	± in%	Ave. of 10 Calc.	Std. of 10 Calc.	Std. in% of 10 Calc.	mass%	±	± in%	Ave. of 10 Calc.	Std. of 10 Calc.	Std. in% of 10 Calc.
Avg. regolith	80.7	2.3	3	72.2	0.4	0	72.3	0.7	1	77.6	0.7	1	76.5	0.5	1
NaCl	0.9	0.11	12	0.5	0.01	2	0.49	0.05	9	0.1	0.02	27	0.4	0.0	8
KCl	0.0	0.00	0	0.1	0.01	10	0.06	0.01	20	0.00	0.00	0	0.0	0.0	0
Mg-sulfates	6.8	0.83	12	12.6	0.3	3	12.6	0.6	5	9.40	0.28	3	9.5	0.3	4
Ca-sulfates	1.2	0.6	50	2.4	0.1	4	2.3	0.2	9	2.0	0.2	10	2.0	0.2	11
Fe-sulfates	0.0	0.00	0	1.8	0.6	31	1.8	0.7	37	0.0	0.00	0	0.0	0.0	0
Ca-phosphate	0.3	0.04	13	0.5	0.01	1	0.43	0.06	13	0.2	0.01	8	0.2	0.1	41
Cr-spinel	0.1	0.01	14	0.2	0.00	1	0.18	0.02	11	0.2	0.00	3	0.2	0.0	9
Ti-ilmenite	0.4	0.04	8	0.5	0.01	1	0.48	0.05	10	0.5	0.01	2	0.5	0.1	10
Hem	3.7	0.6	16	4.0	0.3	8	4.0	0.5	12	5.4	0.2	4	5.4	0.2	3
Qtz	5.8	1.4	25	5.2	0.2	4	5.3	0.4	8	4.8	0.4	9	5.2	0.4	8
χ^2/ν	0.25			0.01			0.04	0.03		0.06			0.10	0.05	
Subtotal sulfates	6.8	0.8	12	16.8	0.7	4	16.8	0.9	5	9.4	0.3	3	9.5	0.3	4
Ratio of Mg-sulfate to Ca-sulfate	6.3	2.8	45	6.0	0.3	4	6.1	0.6	9	5.4	0.5	9	5.3	0.5	10

[a]An average composition from three shallow regolith measurements was used as a component. The Fe-oxides (magnetite and hematite) assigned by Mössbauer analyses were not included. The subtotals of sulfates account only for "added" fractions of sulfates compared to the average composition of shallow regolith.

trench, Table 4) the major "extra" mineral phases are sulfates, mainly Mg-sulfates accompanied by a small amount of Ca-sulfates. The calculation also suggests extra SiO_2 and Fe-bearing materials in the residual compositions (Table 4).

[28] Mass-balance mixing-model calculations using an error-weighted least squares technique [*Korotev et al.*, 1995; *Wang et al.*, 2006] can place tighter constraints on the salt mineralogy than the simplified molar ratio comparison described above. To concentrate on "extra" salts, the composition of averaged-shallow-regolith (disturbed soil samples in rover tracks of sol 122, sol 135, and sol 158) in the vicinity of The Boroughs and the Big Hole was used as one of the model components. Salt phases tested in the mixing model were Na- and K-chlorides, Mg-, Ca-, and Fe-sulfates (the hydration states were not tested since APXS data do not contain information on hydrogen), as well as Ca-phosphate, Fe-Ti-Cr oxides, and SiO_2. A few mass% of Fe were assigned to magnetite and hematite by Mössbauer analyses (Table 2), this mass% of Fe was removed from the regolith composition in the calculations and not shown in Table 5. Further details on mass-balance mixing-model calculation used for the analyses of Gusev soils and rocks are given by *Wang et al.* [2006].

[29] The mineral assemblages (in mass%) that give the best matches (judged by the value of $\chi^2/\nu < 1$ [*Korotev et al.*, 1995]) to the regolith compositions of the Big Hole and The Boroughs trench are listed in Table 5. The results indicate not only the type of salts, but also their relative proportions. For The Boroughs trench, the best matches indicate ~17 wt% of additional sulfates in the wall regolith and ~11 wt% in the floor regolith; less amount of average shallow regolith (~72 wt%) in the wall regolith than in floor regolith (~77 wt%); a higher Mg- to Ca-sulfate molar ratio (~6) in wall regolith than in floor regolith; additional Fe-sulfate in wall regolith but not in floor regolith; very minor amounts of NaCl and KCl in wall regolith and only NaCl in floor regolith. For the regolith within both trenches, Fe_2O_3 and SiO_2 are needed in order to obtain the best compositional matches. For these, additional Fe_2O_3 is supported by Mössbauer analysis according to higher Fe^{3+}/Fe_T values (0.36 and 0.42 within the Boroughs trench, 0.44 within the Big Hole trench). These higher Fe^{3+} values are represented by the nanophase ferric oxide component. No direct mineralogical evidence was found for the extra SiO_2. Nevertheless, basaltic weathering is expected to liberate substantial SiO_2, which can result in the formation of amorphous hydrated silica [*McLennan*, 2003].

[30] A first-order and unambiguous result of the mass-balance analysis is that it identifies the type of mineral assemblages that *cannot account* for the measured composition. This analysis also indicates what mineral assemblages *can account* for the measured compositions. End-member mineral phases are used as the input in the tested mineral assemblages, purposely to cover a wide compositional range. In so doing, the solid solutions of these end-member minerals are all included as potential mineral candidates. Nevertheless, we emphasize that direct mineralogical detection is absolutely essential to demonstrate that these minerals are actually present.

[31] The uncertainties of the mixing-models for the wall and floor regolith within the Big Hole and The Boroughs

trenches are listed in Table 5. These values provide a measure of the goodness of fit for individual mineral phases within each assemblage. These uncertainties were calculated on the basis of the regolith compositions given in Table 3, the chemistry of the input (model) minerals in the assemblages, and weighting factors selected on the basis of the relative standard deviation (SD%) for the APXS data [*Gellert et al.*, 2004, Table 1]. The values of these uncertainties will increase when considering the propagation of the analytical uncertainties (listed in Table 3 with "±" as headers) for each target.

[32] In order to evaluate the sensitivity of modeled mineral proportions, we made another ten sets of mixing-model calculations for the wall regolith and for the floor regolith within The Borough trench respectively, using ten randomly varied compositions for each. These varied compositions follow a normal cumulative distribution using the APXS compositional values in Table 3 as the mean and the accuracy values [*Gellert et al.*, 2004, Table 1] (which are larger than the analytical uncertainties in Table 3) as the standard deviations. The average model proportions from these ten calculations for each target are listed in Table 5; in comparison with the results using APXS compositions of Table 3. Although ten sets of varied compositions are not enough to cover the whole range of compositional variations that may be induced by analytical uncertainties and instrumental accuracy errors, we estimate that the values before the decimal in mass% for mineral proportions in the mixing model results are independent of analytical uncertainties and instrumental accuracy errors for most cases and thus can be taken as representative of the mineral mode of these two regolith compositions.

[33] On the basis of the first-order molar ratio comparison of the cations and anions and the mass-balance mixing-model analysis, significant amounts of salts have been deposited in the deep regolith within the Big Hole and The Boroughs trenches, mainly Mg-sulfates with minor Ca-and Fe-sulfates, trace Na-and K-chlorides, and extra Fe oxides and silica (Table 5).

4.2. Mineralogy of Silicates: Normative Calculation, Mixing-Model, and Olivine Mass% Based on Fe-Only Information

[34] The next question that needs to be answered is whether the additional salts were produced locally from the chemical weathering of silicates, or if they were produced elsewhere and were transported into the trench regolith. An evaluation of the proportional variation of silicate minerals within the salt-free portion of deep regolith relative to general shallow regolith may provide some insight into the degrees of alteration of the basaltic regolith, thus would be helpful to address that question. This analysis may further elucidate the potential processes responsible for the formation and distribution of salts found in the trenches.

[35] The dissolution of igneous minerals during acidic alteration is a potential source of Mg and Ca ions, the building blocks of salts found within the trench regolith. When the fluid-to-rock ratio is low, olivine would likely make the largest contribution to fluid chemistry and alteration mineralogy, given its rapid dissolution rate compared to other rock-forming silicates [*Pokrovsky and Schott*, 2000a, 2000b; *Wogelius and Walther*, 1992]. Experimental evidence indicates that acidic alteration of olivine-bearing basalt tends to produce fluids that are rich in Mg, Fe, and SiO_2, with minor Ca from leaching of pyroxenes or plagioclase [*Tosca et al.*, 2004]. Mg ions were likely released from olivine, accompanied by the precipitation of silica and the oxidation of Fe^{2+} (released from olivine) to ferric-bearing oxides or sulfates (C. Schröder, Evidence for olivine weathering in rocks at Gusev crater, manuscript in preparation, 2006). Mg ions could be transported by the fluids with more mobile elements (S, Cl, Br) and eventually deposited as Mg-sulfates and Mg-chlorides. Ca ions can be leached from pyroxene and feldspar during higher-degree alteration. The transportation of Ca ions by the fluids will be limited, however, by the early precipitation of Ca-sulfate due to its lower solubility than Mg-salts.

[36] On the basis of the concepts and observations discussed above, a decrease in olivine mass% in a basaltic regolith might indicate the effect of acidic alteration. A simple calculation of the variation of olivine mass% within regolith from the top, the wall, and the floor of the two trenches was conducted, and only the information derived from the Fe content and Fe-mineralogy was used. Such information includes the total Fe (mass%) from APXS, the mass% of Fe as Fe^{2+} associated with olivine from Mössbauer data, and the derived Fo_{60} for olivine in typical Gusev rocks and soils based on the correlation between the Mössbauer quadrupole splitting and the measurement temperatures [*Morris et al.*, 2004]. The olivine mass% values so obtained are normalized against the salt-free percentage of each regolith sample, to remove the dilution effect of salt deposition. Figure 7a plots the mass% of olivine in the salt-free portion of the regolith at three trench sites versus the mass% of Fe in nanophase ferric oxides (Fe^{3+}_npOx), which are loosely correlated with the SO_3 concentrations (Figure 7b) and considered to be an indicator of alteration at Gusev [*Morris et al.*, 2005, 2006]. Fo_{60} determined by Mössbauer analysis is in the range of the Mg/(Mg + Fe) ratio (Fo_{51-55}) of olivine in Gusev plain basalts inferred from normative calculations [e.g., *McSween et al.*, 2004, 2006] and by Mini-TES spectral deconvolution [*Christensen et al.*, 2004; *Ruff et al.*, 2005]. The exact Fo value, however, affects the olivine mass% in our calculation. We randomly selected a general compositional range for the olivine in the regolith at the vicinity of the two trenches on the plains, Fo_{55} to Fo_{65}, to be used to determine the potential variation range of olivine mass% in each regolith sample (The vertical error bars in Figure 7a). Compared with the data points from the surface regolith of the Big Hole and The Boroughs (clustered with those from the Road Cut trench at Laguna Hollow at the low end of the Fe^{3+}_npOx values), the decrease in olivine mass% in The Boroughs regolith are almost negligible when taking into account the error bars. A decreasing trend in olivine mass% from the surface to the floor regolith in the Big Hole trench is evident, even taking into account potential errors introduced by Fo variations (Figure 7a).

[37] Knowledge of the complete silicate mineralogy of the salt-free portion of regoliths is needed to assess the proportional variations of major igneous minerals (olivine, pyroxene and feldspar) and the potential degree of acidic

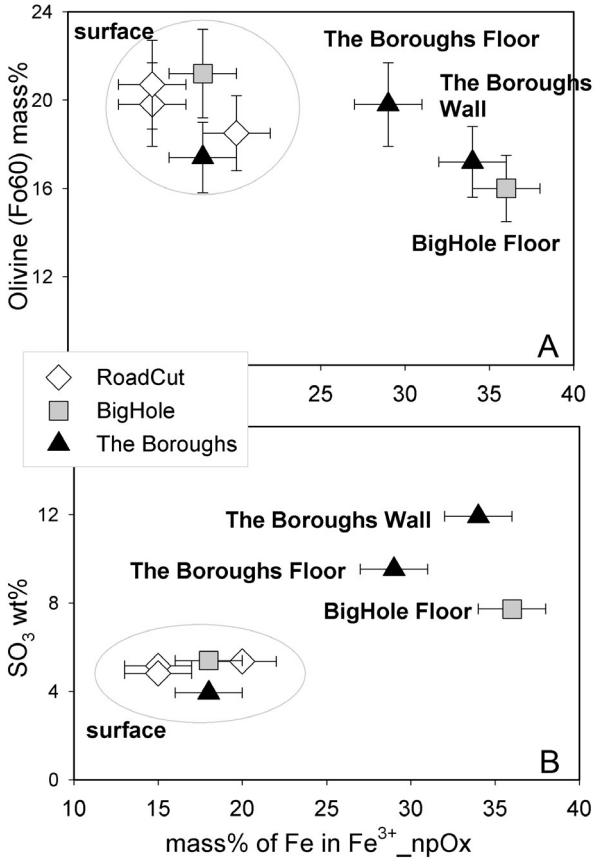

Figure 7. (a) The olivine mass% in the salt-free portion of regolith of the three trenches calculated using Fe-only information from the APXS (Fe mass%) and MB (Fe^{2+}_Ol and Fo_{60}). Vertical error bars in Figure 7a represent calculation results when covering a range from Fo_{55} to Fo_{65} (the rest of the error bars in Figures 7a and 7b represent the analytical uncertainties of the APXS and Mössbauer analyses). The regolith targets within the Big Hole trench (gray squares) show a decrease trend in the olivine mass%. The olivine mass% values are plotted against the mass% of Fe in ferric nanophase oxides (Fe^{3+}_np) in Figure 7a. (b) The proportion of ferric nanophase oxides correlates positively with SO_3 concentrations and is considered to be the primary alteration product on the Gusev plains.

weathering [*Tosca et al.*, 2004]. Our attempt to obtain this information using normative analysis and mass-balance mixing-model calculations provides ambiguous results. The silicate mineralogy obtained from normative calculations is largely affected by the relatively significant analytical uncertainty in Na concentrations [*Gellert et al.*, 2004]. This uncertainty affects the proportion of Na-feldspar and thus the amount of Si taken by this mineral, which in turn affects the relative proportions of olivine and pyroxene. The proportional variations of silicates obtained by normative analysis show no trends. The Na analytical uncertainty has less of an effect on mass-balance mixing-models. Because all mineral components are calculated simultaneously, and we have used a large weighting factor (20 mass% in concentration) for Na, the calculation results are not driven by Na concentrations. The olivine proportions for two regolith samples at the Big Hole and three regolith samples at The Boroughs obtained from mixing-models show a similar variation pattern to Figure 7a, i.e., a slight decrease (<5%) in the proportion of olivine in the floor regolith within Big Hole, and a similar variation pattern as in Figure 7a for The Boroughs (not shown). There are no variation trends in the proportions of feldspar and pyroxene. Note that small amounts of SiO_2 are needed in both normative analysis and mixing-model calculations to match the regolith compositions at both trench sites.

[38] In principle, we can compare the proportions of silicate minerals extracted from Mini-TES spectral deconvolution with the results of the above calculations. The Mini-TES spectra are remarkably consistent for the disturbed soils at Gusev Crater, with the trench materials showing little mineralogical variability from near-surface disturbed soils. The olivine mass% derived from a Mini-TES spectrum of the sol 089 disturbed soil [*Christensen et al.*, 2004] agrees well with the value derived from the mass-balance mixing-model calculation for the shallow subsurface regolith composition averaged over three measurements (Figure 8), and also with the olivine mass% value (within uncertainties) from the direct olivine calculation using the Fe-only information. The discrepancies in pyroxene and feldspar proportions are larger, but still within (or nearly within) the range defined by the relative uncertainty in Mini-TES spectral deconvolution.

[39] In general, our analyses strongly suggest deposition of sulfates, mainly Mg-sulfates accompanied by Ca-sulfates and perhaps Fe-sulfates, within the regolith exposed by the Big Hole and The Boroughs trenches. Iron is more oxidized in the subsurface regolith than in the regolith at the trench surface. An excess of SiO_2 within all plains trench regolith samples is inferred. On the basis of these analyses, the degree of alteration of igneous minerals within trench regolith is difficult to ascertain, but is probably low. Our analyses are consistent with a slight decrease in the proportion of olivine in the floor regolith of the Big Hole trench compared to the shallow regolith,

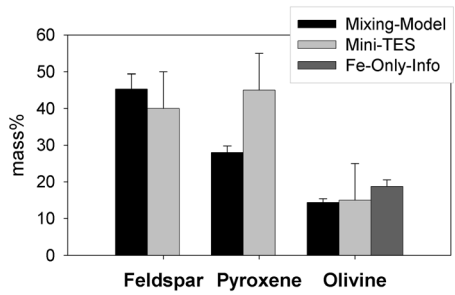

Figure 8. Major silicate mineral proportions in the salt-free component of shallow subsurface regolith exposed in rover tracks, as obtained from two calculations, are compared with the silicate mineralogy extracted from Mini-TES spectral deconvolution. The error bars represent the Fo_{55} – Fo_{65} compositional range for mass% olivine calculation using Fe-only information and the uncertainties in the mixing model calculation and in Mini-TES spectral deconvolution.

Table 6. Normative "Equivalent" Olivine mole% in Regolith When Converted From Mg-Sulfates, Showing the Excess of Mg in These Trench Regolith Materials Relative to Averaged Shallow Regolith and Abraded Adirondack Rock

	Olivine in mole%	Mg/(Mg + Fe) of Olivine
The Boroughs trench wall regolith	34.0	68
The Boroughs trench floor regolith	30.2	63
The Big Hole trench floor regolith	24.5	62
Average shallow regolith on the plains	23.8	56
Abraded plain basalt (Adirondack rock)	29.4	48

whereas variation in olivine abundance at The Boroughs appears to be negligible.

5. Discussion

5.1. Deposition Mechanism

[40] We consider three hypotheses for the formation of the salt-rich subsurface regolith at The Boroughs and Big Hole trenches: (1) multiple episodes of acidic fluid infiltration, accompanied by in situ interaction with igneous minerals and salt deposition; (2) an open hydrologic system characterized by ion transportation in the fluid, subsequent evaporation of the fluid and salt deposition; and (3) emplacement and mixing of impact ejecta of variable composition.

[41] In contrast to the mineral compositions of evaporite salts commonly observed on Earth [*Kinsman*, 1974], the deposited sulfates inferred from the trench regolith compositions have low Ca/Mg ratios. The high Ca/Mg ratios typically observed for terrestrial evaporites result from the dominance of feldspar alteration during weathering of the Earth's granodioritic upper continental crust. The experimental results of *Tosca et al.* [2004] demonstrate that during weathering of olivine-bearing basalt under condition appropriate to Mars, production of fluids with low Ca/Mg ratio can occur under conditions of low pH and low water to rock ratio as a result of the dominance of olivine dissolution under these conditions. The presence of a Mg-sulfate dominated mineralogy in the trench regolith is consistent with a formation process involving in situ alteration of olivine-bearing basaltic soil followed by evaporation to form a Mg-sulfate dominated salt mineralogy. The persistence of basaltic mineralogy with a minor decrease in olivine content suggests that if in situ alteration of soil in the trenches took place, it was not very extensive (i.e., the water-to-rock ratio was low). A high Mg/Ca would also preclude a significant amount of aqueous "flushing" of the salts precipitated after the alteration event(s), since such flushing would be likely to preferentially remove highly soluble Mg-sulfates, and leave behind less soluble Ca-sulfates.

[42] An observation that argues against an in situ alteration process is the lack of obvious crusty materials within the two trenches. Another observation against a closed-system in situ alteration process is the fact that we can infer an excess of Mg in the trench regolith (especially at The Boroughs), as follows. If the Mg-sulfate present in the trench regolith was formed via in situ alteration of olivine-bearing soil under conditions similar to those discussed above, then converting (using the number of moles of Mg) the Mg ions in the evaporite component (Mg-sulfates) of the trench regolith back to an equivalent amount of Mg-olivine should yield an amount of olivine very similar to that of a typical Gusev regolith. When this calculation was made (Table 6) for the wall regolith at The Boroughs trench (richest in S), the "equivalent" olivine (~34 mole%) is significantly higher than that of a typical Gusev shallow regolith (~24 mole%). This value is even higher than the olivine content (~29 mole%) in the abraded rock Adirondack (a plains basalt having the highest olivine content). That is to say if assuming that the "initial regolith" at The Boroughs is generated by physical erosion (impact/aeolian) of Gusev basalts similar in composition to Adirondack, then this regolith would not contain enough Mg to produce the abundance of Mg-sulfate found by Spirit within The Boroughs trench. This calculation suggests that there may be an external source for the "excess" cations, especially Mg.

[43] The inference of excess-Mg in trench regolith suggests that some or all of the excess cations could have been transported in by fluid from outside of the trench, i.e., trench soils may have been affected by an open hydrologic system. The low Ca/Mg ratio observed in trench regolith could result from ion transportation by fluid accompanied by evaporation and sequential salt deposition. In order to spatially separate Mg-salts from Ca-salts, an open system hydrologic hypothesis would require more fluid to be involved, in which both Ca and Mg were available in the source region. Because of the difference in solubility of Mg- and Ca-sulfate, Mg cations would be carried preferentially by the fluids, while Ca-sulfates were deposited elsewhere. This hypothesis does not set a limit on the degree of alteration of igneous materials at the source region for the alteration fluid. This hypothesis does imply, however, that a minimum amount of alteration of igneous minerals has occurred within the regolith where the salt was deposited. Because the residual altered basaltic minerals (from which Mg and Ca were derived) would have been left behind, only the fluids enriched in Mg^{2+}, Fe^{2+} (and Fe^{3+}) and SO_4^{2-} (and HSO_4^-) reached the trench site.

[44] The open system hydrologic hypothesis seems adequate to interpret the geochemical observations and the analysis results for The Boroughs trench regoliths, where the large amounts of excess-Mg are observed and minimal alteration of silicate minerals is implied. At the Big Hole trench site, on the basis of the observation of a decreasing trend in olivine content (Figure 7a) and no obvious excess-Mg (Table 6), the in situ interaction may have happened, but may not be the only process involved.

[45] We do not have the data to constrain the spatial scale of this open system, or the direction of fluid movement. During vertical migration (by capillary action) and evaporation, Ca-sulfates may have deposited at depths not reached by the trench excavations, whereas the much more soluble components, Mg^{2+}, SO_4^{2-}, and Br^- were progressively concentrated at the uppermost levels. The separation of Mg from Ca could also occur during lateral transportation driven by topographic differences, with sequential evaporation occurring along the way. This situation might result in the accumulation of Mg^{2+}, SO_4^{2-}, and Br^- - enriched fluids in topographic lows and eventual deposition of Mg-

sulfates during late-stage evaporation. Ca-rich sulfates might precipitate higher in the topographic section under such a scenario due to their relatively lower solubility compared to Mg-sulfates. We note that Ca-sulfates have been inferred to be present by a compositional trend (r = 0.963) found in the compositions of six abraded rocks on West Spur [*Ming et al.*, 2006; *Wang et al.*, 2006]. West Spur is a westward projecting salient of ~8–26 m above the elevation of The Boroughs trench site [*Arvidson et al.*, 2005, Figure 4].

[46] A third hypothesis for the formation of the salty regolith at two trench sites is that it was delivered to the site from some distance as impact ejecta. Craters and rocks emplaced by impact are seen everywhere at Gusev along Spirit's traverse to the Columbia Hills. The effect of impact gardening is seen in the microscopic images of the regolith within the Big Hole and The Boroughs trenches. While the impact process may be one of the causes contributing to the poorly sorted nature of the trench regolith, it is less likely to affect the chemical signatures there. The MgO versus SO_3 and Al_2O_3 versus SO_3 correlations seen from three data points at the Big Hole trench site have similar slopes as those from the data at The Boroughs trench site (Figures 3a and 3b). These similarities in compositional correlations from two targets of 1.2 km apart suggest that they are the products of a similar chemical process (possibly at different scales, and at different times), but probably not by physical mixing, which would tend to homogenize the chemical composition in regolith.

[47] Variations in salt concentrations and the degrees of oxidation (Fe^{3+}/Fe_T) were observed at different depths within the Boroughs trench (Table 5, Table 2). Since stratigraphic layering cannot be extracted confidently from only three measurement spots, impact gardening (after-salt-deposition) cannot be excluded as a cause of the heterogeneity. The contributions from acidic fluid transportation could also be one of the causes: i.e., a thermal gradient near the regolith surface could induce the upward migration of the brine; the evaporation of the brine could be followed by the deposition of salts at the surface. The aeolian process would homogenize the uppermost layer of surface dust and would leave the most salt-rich regolith at some shallow depth, as observed in the wall regolith within The Boroughs trench.

[48] It is possible that these mechanisms, coupled with some level of reworking of deposits by eolian processes, may all have affected some aspects of the current regolith at the two trench sites at different times. The impact events may have mainly affected the emplacement and gardening of regolith at the trench sites, while fluid transportation and evaporation would be the major controlling factors for the salt chemistry and mineralogy observed by Spirit.

5.2. Inferred Fluid Properties

[49] The high concentrations of S, Cl, and Br, the coupling and decoupling (at The Boroughs) of Cl from S, and the large variation in Br concentrations indicate that the parent acidic fluids must have highly variable compositions. Multiple episodes of fluid (liquid or vapor) to rock interactions, ion transportation, and repetitious precipitation and evaporation would all be reasonable sources. In addition, the low fluid-to-rock ratios would enhance the variations.

[50] Bromine is highly mobile compared to Cl and S, because of the extremely high solubility of bromides in aqueous solution: double that of chlorides, and three to four times that of sulfates. Even if Br originated from the same sources as Cl and S (e.g., as volatiles from volcanic activity), it can be collected in a trace amount of water, such as in transient water from melting of frost or ice, and then to be moved and redeposited at locations away from the chloride and sulfate deposition sites [*Yen et al.*, 2005]. High Br concentrations were found in the interior of the plains basalts [*Gellert et al.*, 2004], and these occurrences were considered possibly to be deposited from the last stage of brines [*Haskin et al.*, 2005], which diffused into the rock interior through a network of veins and vugs (as observed in microscopic images of abraded Mazatzal [*Herkenhoff et al.*, 2004]). The movement of Br in regolith would follow the same path [*Yen et al.*, 2005], i.e., it could be collected and transported by trace amounts of water and deposited from the last drop of brine during evaporation. Thus highly variable Br concentrations in surface soils, shallow regoliths, and the subsurface regolith within the Big Hole trench (Figure 3d) would be consistent with episodic fluid migration and evaporation (even with trace amounts).

[51] Much higher Br concentrations (Figure 3d) in the regolith within The Boroughs trench, however, may result from a more effective Br collection by the involvement of larger amounts of aqueous fluids. The highest Br concentrations found in the wall regolith accompanied with the highest S and Mg concentrations would indicate the last stage of dehydration, for which a relatively low fluid to regolith ratio would be implied.

[52] Ratios of S to Cl are nearly constant for all rocks and soils analyzed through sol 156 at Gusev, including "as is" and brushed rock surfaces, the surface soils, shallow regolith exposed in rover tracks, and the deep regolith within the Big Hole trench (Figure 3c). Uniform S/Cl ratios in various near-surface targets are consistent with a smaller solubility difference between S and Cl when comparing with those of S and Br, thus Cl is not as soluble as Br to be collected and moved by tiny amounts of fluids. More importantly, the unvarying S/Cl ratios indicate a similarity in the evaporation processes, and similar S/Cl ratios in initial fluids. For example, $MgSO_4$, NaCl, and KCl have quite similar solubility in water (35.7, 36.0, and 35.5 g/100g water respectively, as binary system [*Lide*, 2001]); if there were equivalent Mg^{2+}, Na^+, and K^+ supply in the aqueous fluids, the major controlling factor on the ratio of deposited sulfates to chlorides would be the S to Cl molar ratios of the initial fluids. Therefore the nearly uniform S/Cl ratios in the deposits reflect a narrow range of S/Cl ratios in the initial fluids.

[53] The deep regolith within The Boroughs trench, however, is one of the exceptions (another one is the multilayer coating on Mazatzal rock [*Haskin et al.*, 2005, Figure 3c]), having a S to Cl molar ratio that doubled the typical values observed elsewhere (Figure 3c). This difference is an indicator of variations, either in the mechanism of salt deposition or in the properties of the fluids involved. We suggest that this phenomenon is directly related to the excess of Mg: when an excess of Mg (over Na and K when comparing with other Gusev targets) exists in the initial fluids, even the fluids may still hold a S to Cl molar ratio

similar to those that reacted with other Gusev targets, the solubility difference of $MgSO_4$ and $MgCl_2$ ($MgCl_2$ has a solubility of 56.0g/100g water, [*Lide*, 2001] as binary system, ~1.5 times more soluble than $MgSO_4$), would have been the major factor that affects the deposition sequence and the S/Cl ratio in the end product. Therefore the Mg-sulfates would be the dominant precipitates relative to Mg-chlorides at The Boroughs, and thus accounting for the high S to Cl ratios in these regolith materials (Figure 3c).

[54] Another influencing factor would be the scale of the region being affected by the acidic fluids during a fluid-regolith-interaction event, which would affect the locations where salts of different types precipitated and the distances between them. The size of the affected region depends on the fluid quantity, the freezing-point depression that would keep the acidic fluids in liquid form even at low temperatures, the brine salinity that affects the freezing-point depression [*Clark et al.*, 2005], the porosity (and stratigraphic structure) of the regolith which determines the path length or depth of fluid migration, and (indirectly) the lateral size of the affected area. When considering multiple episodes of fluids, their evaporation and related salt deposition. All these factors could have affected the concentrations of S, Cl, Br and their spatial distribution within the regoliths at the two trench sites on the plains.

5.3. Water Abundance

[55] Mg-sulfate (kieserite $MgSO_4 \cdot H_2O$), Ca-sulfates (gypsum $CaSO_4 \cdot 2H_2O$, bassanite $CaSO_4 \cdot 1/2H_2O$) and polyhydrate sulfates have been identified at many locations on Mars by the OMEGA spectrometer on the Mars Express spacecraft [*Arvidson et al.*, 2005; *Bibring et al.*, 2005; *Gendrin et al.*, 2005]. Using both fast and epithermal neutron data, the Gamma-Ray Spectrometer on the Mars Odyssey spacecraft detected about 3–8 mass% of water-equivalent-hydrogen (WEH) in the vicinity of Gusev crater with a foot print of ~600 km [*Feldman et al.*, 2005].

[56] Sulfates make up more than 20 mass% of the wall regolith within The Boroughs trench, including the portion in the general shallow regolith and those formed by additional deposition. We are unaware of any experimental evidence that would constrain the type of cation that is bonded to the sulfates in the general shallow regolith at Gusev. On the basis of OMEGA observations, Mg and Ca are the most likely candidates. In a first approximation, if the sulfates within the wall regolith at The Boroughs trench are all highly dehydrated Mg-sulfates (kieserite $MgSO_4 \cdot H_2O$, or amorphous $MgSO_4 \cdot 1.2\text{-}2H_2O$ from dehydration of other hydrous phases [*Vaniman et al.*, 2004]), the structural water in these sulfates would only constitute up to 3–4 mass% of entire regolith at that location. By adding some water trapped in the interstitial spaces among soil grains, the water content of the regoliths within The Boroughs trench just reaches the middle of the range observed by the Odyssey GRS.

[57] Nevertheless, the regolith at The Boroughs trench contains the highest concentration of sulfates measured on the plains (from the landing site to the foot of the Columbia Hills) investigated by Spirit. Thus either some areas with high water concentrations occur that have not yet been found by the rover at the Gusev site (e.g., deeper than 10–11 cm or in some other locations within the GRS footprint), or the Mg-sulfates in the near surface are in a higher hydration state than is stable at the surface under current Mars atmospheric conditions. Recent experimental studies [*Bish et al.*, 2003; *Chipera et al.*, 2005; *Chou and Seal*, 2003, 2005; *Emons et al.*, 1990; *Vaniman et al.*, 2004] suggest that highly hydrated Mg-sulfates could have formed and been retained at the moderate relative humidity and warmer temperatures expected for Mars during periods of high obliquity [*Richardson and Mischna*, 2005]. Some of the Mg sulfate hydrates (e.g., starkeyite $MgSO_4 \cdot 4H_2O$) have stability fields that could be expanded by metastability to allow their persistence where lower hydrates might be anticipated [*Chipera et al.*, 2005; *Wang et al.*, 2005a]. If that is the case at Gusev, the upper limit of water abundance of wall regolith within The Boroughs trench would be ~11 mass% in a first order approximation. Further understanding of this issue requires detailed analyses of more data from MER, OMEGA, and GRS, as well as simulation experiments in laboratories.

6. Conclusion

[58] The Investigations using the full Athena instrument payload on the Spirit rover revealed a highly oxidized sulfur-rich subsurface regolith within the two trenches excavated on the plains, between Bonneville crater and Columbia Hills, during the early part of the extended mission (through sol 156). Data analyses based on the compositional and mineralogical correlations indicate deposition of sulfates, mainly Mg-sulfates accompanied by Ca-sulfates and perhaps Fe-sulfates. The sulfates constitute more than 20 mass% of the subsurface regolith at the Boroughs trench sites. Excesses of Fe_2O_3 and SiO_2, and minor olivine dissolution are also inferred. After evaluating the three hypotheses suggested for the source, formation process, and the current distribution of sulfates within the regolith, we conclude that although there may be multiple contributions to the current chemical state of the regolith, an open hydrologic system, characterized by ion transportation in fluids from sources laterally or at depth, fluid evaporation, and sequential salt deposition, are the most likely mechanisms responsible for the mineralogy and chemistry of the regolith observed by the Spirit rover.

[59] **Acknowledgments.** We thank the NASA Mars program for supporting our participation in the Mars Exploration Rover mission. We thank the management and the engineering team at the Jet Propulsion Laboratory for their innovative and dedicated handling of the rover. We thank the members of the Athena science instrument teams for providing excellent data products. We thank Robert Sullivan and Jeff Biesiadecki for their efforts in developing the trench techniques and for commanding the Spirit rover to actually dig these trenches. Larry A. Haskin passed away during the preparation of this manuscript. We all appreciated very much his guidance during MER operations and data analyses. The MER mission was a stronger one because of his contributions. We thank Bill Feldman of the GRS team (Mars Odyssey) for providing WEH data from Gusev. We thank S. J. Wentworth and three anonymous reviewers for their constructive comments and suggestions; they helped to strengthen this paper.

References

Arvidson, R. E., et al. (2004), Localization and physical properties experiments conducted by Spirit at Gusev crater, *Science*, *305*, 821–824.

Arvidson, R. E., F. Poulet, J.-P. Bibring, M. Wolff, A. Gendrin, R. C. Morris, J. J. Freeman, Y. Langevin, N. Mangold, and G. Bellucci (2005), Spectral reflectance and morphologic correlations in eastern Terra Meridiani, Mars, *Science*, *307*, 591–1593, doi:10.1126/science.1109509.

Bell, J. F., III, et al. (2003), Mars Exploration Rover Athena Panoramic Camera (Pancam) investigation, *J. Geophys. Res.*, *108*(E12), 8063, doi:10.1029/2003JE002070.

Bell, J. F., III, et al. (2004), Pancam multispectral imaging results from the Spirit rover at Gusev crater, *Science*, *305*, 800–806.

Bibring, J.-P., et al. (2005), Mars surface diversity as observed by the OMEGA/Mars Express investigation, *Science*, *307*, 1576–1581, doi:10.1126/science.1108806.

Bish, D. L., J. W. Carey, D. T. Vaniman, and S. J. Chipera (2003), Stability of hydrous minerals on the Martian surface, *Icarus*, *164*, 96–103, doi:10.1016/s0019-1035(03)00140-4.

Boynton, W. V., et al. (2002), Distribution of hydrogen in the near surface of Mars: Evidence for subsurface ice deposits, *Science*, *297*, 81–85.

Chipera, S. J., D. T. Vaniman, D. L. Bish, J. W. Carey, and W. C. Feldman (2005), Experimental stability and transformation kinetics of magnesium sulfate hydrates that may be present on Mars, *Lunar Planet. Sci.*, *XXXVI*, abstract 1497.

Chou, I.-M., and R. R. Seal II (2003), Determination of epsomite-hexahydrite equilibria by the humidity-buffer technique at 0.1 MPa with implications for phase equilibria in the system $MgSO_4$–H_2O, *Astrobiology*, *3*, 619–629.

Chou, I.-M., and R. R. Seal (2005), Determination of goslarite-bianchite equilibria by the humidity-buffer technique at 0.1 MPa, *Chem. Geol.*, *215*, 517–523.

Christensen, P., and S. T. Harrison (1993), Thermal infrared emission spectroscopy of natural surfaces: Application to desert varnish coatings on rocks, *J. Geophys. Res.*, *98*, 19,819–19,834.

Christensen, P. R., et al. (2003), Miniature Thermal Emission Spectrometer for the Mars Exploration Rovers, *J. Geophys. Res.*, *108*(E12), 8064, doi:10.1029/2003JE002117.

Christensen, P. R., et al. (2004), Initial results from the Mini-TES experiment in Gusev crater from the Spirit rover, *Science*, *305*, 837–842.

Clark, B. C., et al. (2005), Results and implications of mineralogical models for chemical sediments at Meridiani Planum, *Lunar Planet. Sci.*, *XXXIV*, abstract 1446.

Crumpler, L. S., et al. (2005), Mars Exploration Rover geologic traverse science by the Spirit rover in the plains of Gusev crater, Mars, *Geology*, *33*(10), 809–812.

Emons, H. H., G. Ziegenbalg, R. Naumann, and F. Paulik (1990), Thermal decomposition of the magnesium sulphate hydrates under quasi-isothermal and quasi-isobaric conditions, *J. Thermal Anal.*, *36*, 1265–1279.

Farrand, W. H., J. F. Bell III, J. R. Johnson, S. W. Squyres, J. Soderblom, and D. W. Ming (2006), Spectral variability among rocks in visible and near-infrared multispectral Pancam data collected at Gusev crater: Examinations using spectral mixture analysis and related techniques, *J. Geophys. Res.*, *111*, E02S15, doi:10.1029/2005JE002495.

Feldman, W. C., et al. (2005), Topographic control of hydrogen deposits at mid- to low latitudes of Mars, *Lunar Planet. Sci.*, *XXXVI*, abstract 1328.

Fergason, R. L., P. R. Christensen, J. F. Bell III, M. P. Golombek, K. E. Herkenhoff, and H. H. Kieffer (2006), Physical properties of the Mars Exploration Rover landing sites as inferred from Mini-TES derived thermal inertia, J. Geophys. Res., *111*, E02S21, doi:10.1029/2005JE002583.

Gellert, R., et al. (2004), Chemistry of rocks and soils in Gusev crater from the Alpha Particle X-Ray spectrometer, *Science*, *305*, 829–832.

Gendrin, A., et al. (2005), Sulfates in Martian layered terrains: The OMEGA/Mars Express View, *Science*, *307*, 1587–1591, doi:10.1126/science.1109087.

Golombek, M. P., et al. (2006), Geology of the Gusev cratered plains from the Spirit rover transverse, *J. Geophys. Res.*, *111*, E02S07, doi:10.1029/2005JE002503.

Grant, J. A., et al. (2006), Crater gradation in Gusev crater and Meridiani Planum, Mars, *J. Geophys. Res.*, *111*, E02S08, doi:10.1029/2005JE002465.

Haskin, L. A., et al. (2005), Water alteration of rocks and soils from the Spirit rover site, Gusev crater, Mars, *Nature*, *436*, 66–69.

Herkenhoff, K. E., et al. (2003), Athena Microscopic Imager investigation, *J. Geophys. Res.*, *108*(E12), 8065, doi:10.1029/2003JE002076.

Herkenhoff, K. E., et al. (2004), Texture of the soils and rocks at Gusev crater from Spirit's Microscopic Imager, *Science*, *305*, 824–826.

Kinsman, D. J. J. (1974), Calcium sulphate minerals of evaporite deposits: Their primary mineralogy, in *Fourth Symposium on Salt*, vol. 1, edited by A. H. Coogan, pp. 343–348, North. Ohio Geol. Soc., Cleveland.

Klingelhöfer, G., et al. (2003), Athena MIMOS II Mössbauer spectrometer investigation, *J. Geophys. Res.*, *108*(E12), 8067, doi:10.1029/2003JE002138.

Korotev, R. L., L. A. Haskin, and L. B. Jolliff (1995), A simulated geochemical rover mission to the Taurus Littrow valley of the Moon, *J. Geophys. Res.*, *100*, 14,403–14,420.

Lide, D. R. (2002), *Handbook of Chemistry and Physics*, pp. 4–67 to 4–84, CRC Press, Boca Raton, Fla.

McLennan, S. M. (2003), Sedimentary silica on Mars, *Geology*, *31*, 315–318.

McSween, H. Y., et al. (2004), Basaltic rocks analyzed by the Spirit rover in Gusev crater, *Science*, *305*, 842–845.

McSween, H. Y., et al. (2006), Characterization and petrologic interpretation of olivine-rich basalts at Gusev Crater, Mars, *J. Geophys. Res.*, *111*, E02S10, doi:10.1029/2005JE002477.

Ming, D. W., et al. (2006), Geochemical and mineralogical indicators for aqueous processes in the Columbia Hills of Gusev crater, Mars, *J. Geophys. Res.*, *111*, E02S12, doi:10.1029/2005JE002560.

Morris, R. V., et al. (2000), Mineralogy, composition, and alteration of Mars Pathfinder rocks and soils: Evidence from multispectral, elemental, and magnetic data on terrestrial analogue, SNC meteorite, and Pathfinder samples, *J. Geophys. Res.*, *105*, 1757–1817.

Morris, R. V., et al. (2004), Mineralogy at Gusev crater from the Mössbauer spectrometer on the Spirit rover, *Science*, *305*, 833–836.

Morris, R. V., D. W. Ming, B. C. Clark, G. Klingelhoefer, R. Gellert, D. Rodionov, C. Schroeder, P. de Souza, A. Yen, and the Athena Science Team (2005), Abundance and speciation of water and sulfate at Gusev crater and Meridiani Planum, *Lunar Planet. Sci.*, *XXXVI*, abstract 2239.

Morris, R. V., et al. (2006), Mössbauer mineralogy of rock, soil, and dust at Gusev crater, Mars: Spirit's journey through weakly altered olivine basalt on the Plains and pervasively altered basalt in the Columbia Hills, *J. Geophys. Res.*, doi:10.1029/2005JE002584, in press.

Pokrovsky, O., and J. Schott (2000a), Forsterite surface composition in aqueous solutions: A combined potentiometric electrokinetic, and spectroscopic approach, *Geochim. Cosmochim. Acta*, *64*, 3299–3312.

Pokrovsky, O., and J. Schott (2000b), Kinetics and mechanism of forsterite dissolution at 25C and pH from 1 to 12, *Geochim. Cosmochim. Acta*, *64*, 3313–3325.

Richardson, M. I., and M. A. Mischna (2005), Long-term evolution of transient liquid water on Mars, *J. Geophys. Res.*, *110*, E03003, doi:10.1029/2004JE002367.

Rieder, R., R. Gellert, J. Brückner, G. Klingelhöfer, G. Dreibus, A. Yen, and S. W. Squyres (2003), The new Athena alpha particle X-ray spectrometer for the Mars Exploration Rovers, *J. Geophys. Res.*, *108*(E12), 8066, doi:10.1029/2003JE002150.

Ruff, S. W., P. R. Christensen, and the Athena Science Team (2005), The rocks of Gusev crater as viewed by MiniTES, *Lunar Planet. Sci.*, *XXXVI*, abstract 2155.

Squyres, S. W., et al. (2003), Athena Mars rover science investigation, *J. Geophys. Res.*, *108*(E12), 8062, doi:10.1029/2003JE002121.

Squyres, S. W., et al. (2004), The Spirit rover's Athena Science Investigation at Gusev crater, Mars, *Science*, *305*, 794–799.

Tosca, N. J., S. M. McLennan, D. H. Lindsley, and M. A. A. Schoonen (2004), Acid-sulfate weathering of synthetic Martian basalt: The acid fog model revisited, *J. Geophys. Res.*, *109*, E05003, doi:10.1029/2003JE002218.

Vaniman, D. T., D. L. Bish, S. J. Chipewa, C. I. Fialips, J. W. Carrey, and W. C. Feldman (2004), Magnesium sulphate salts and the history of water on Mars, *Nature*, *431*, 663–665.

Wang, A., L. A. Haskin, S. W. Squyres, R. Arvidson, L. Crumpler, R. Gellert, J. Hurowitz, C. Shroeder, N. J. Tosca, and the Athena Science Team (2004), Chemistry and mineralogy of the regolith at the Gusev plains, *Eos Trans. American Geophysical Union*, *85*(47), Fall Meet. Suppl., Abstract P21A–0220.

Wang, A., J. Freeman, B. T. Greenhagen, and B. L. Jolliff (2005a), Raman spectra of hydrated Mg- and Ca-sulfates and field testing the Mars Microbeam Raman Spectrometer (MMRS), paper presented at Geological Society of America Annual Meeting and Exposition, Salt Lake City.

Wang, A., et al. (2005b), Sulfate deposition in regolith exposed in trenches on the plains between the Spirit landing site and Columbia Hills in Gusev crater, *Mars, Lunar Planet. Sci.*, *XXXVI*, abstract 2236.

Wang, A., et al. (2006), Evidence of phyllosilicates in Wooly Patch, an altered rock encountered at West Spur, Columbia Hills, by the Spirit rover in Gusev Crater, Mars, J. Geophys. Res., *111*, E02S16, doi:10.1029/2005JE002516.

Wogelius, R., and J. Walther (1992), Olivine dissolution kinetics at near-surface conditions, *Chem. Geol.*, *97*, 101–112.

Yen, A. S., S. S. Kim, M. H. Hecht, M. Frant, and B. Murray (2000), Evidence that the reactivity of the Martian soil is due to superoxide ions, *Science*, *289*, 1909–1912.

Yen, A. S., et al. (2005), An integrated view of the chemistry and mineralogy of Martian soils, *Nature*, *436*, 49–54, doi:10.1038/nature03637.

R. Anderson, Jet Propulsion Laboratory, California Institute of Technology, 4800 Oak Grove Drive, Pasadena, CA 91109, USA.

L. Crumpler, New Mexico Museum of Natural History and Science, 1801 Mountain Road, Albuquerque, NW 87104, USA.

W. H. Farrand, Space Science Institute, 4750 Walnut Street, Boulder, CO 80301, USA.

R. Gellert, Abteilung Kosmochemie, Max-Planck-Institut für Chemie, Postfach 3060, D-55020 Mainz, Germany.

K. Herkenhoff, U. S. Geological Survey, 2255 North Gemini Drive, Flagstaff, AZ 86001, USA.

J. Hurowitz and N. J. Tosca, Department of Geosciences, State University of New York, Stony Brook, NY 11794-2100, USA.

B. L. Jolliff and A. Wang, Department of Earth and Planetary Sciences, Washington University, Campus Box 1169, One Brookings Drive, St. Louis, MO 63130, USA. (alianw@levee.wustl.edu)

A. T. Knudson, Department of Geological Sciences, Arizona State University, Box 876305, Tempe, AZ 85287, USA.

C. Schröder, Institut für Anorganische und Analytische Chemie, Johannes Gutenberg-Universität, Staudinger Weg 9, D-55128 Mainz, Germany.

S. W. Squyres, Department of Astronomy, Cornell University, 428 Space Science Building, Ithaca, NY 14853, USA.